The mechanical behaviour of compacted Lambeth-group clays with and without fibre reinforcement

Abdullah Ekinci

Assistant Professor, Civil Engineering Program, Middle East Technical University, Northern Cyprus Campus, Kalkanli, Guzelyurt, North Cyprus, via Mersin 10, Turkey Email: ekincia@metu.edu.tr, ORCID number: 0000-0002-6787-9983, Tel.: +90 392 661 2925, Fax: +90 392 661 2999

Pedro Miguel Vaz Ferreira

Associate Professor, University College London, Gower Street, WC1E 6BT, London/UK. E-mail: p.ferreira@ucl.ac.uk, ORCID number: 0000-0002-4626-7443

Mohammadreza Rezaeian

PhD Graduate in Geotechnical Engineering, University College London, Gower Street, WC1E 6BT, London/UK. E-mail: m.rezaeian.12@ucl.ac.uk

Abstract

This study investigated the effect of fibre reinforcement on the large strain behaviour of compacted clay samples tested using large triaxial test equipment. A novel specimen preparation method was proposed where peds of clay are compacted to closely simulate the in-situ compaction. A large number of 100 × 200 mm triaxial tests and one-dimensional compression tests were performed using reinforced and unreinforced samples. The behaviour of unreinforced samples was observed to be similar to highly fissured clays; ped compaction generated a random fissure pattern due to the contact between peds. The addition of fibres to the compacted samples created fissures with higher mobility at lower friction than those in the unreinforced samples; hence, the state boundary surface of reinforced clay was below that of the unreinforced clay. With the addition of fibres, the failure mechanism changed from the formation of a shear plane to barrelling, demonstrating that the fibres transferred stresses further away from the shear plane, producing a more homogeneous stress distribution. The preparation method proposed here produced a fissure pattern in the clay that introduced transitional behaviour, which was drastically reduced with addition of the fibres, allowing better normalisation and the definition of a unique boundary surface.

Keywords

Fabric, Structure, Laboratory Tests, Reinforced Soil, State Boundary Surface, Fissured Clay

List of notations

OMC	optimum moisture content
MDD	maximum dry density
NCL	normal compression line
iso-NCL	isotropic normal compression line
INCL*	isotropic normal compression line of the reconstituted clay
CSL	critical state line
SBS	state boundary surface
SBS*	intrinsic state boundary surface
LBS	local boundary surface
v	specific volume
p`	mean effective stress
N	specific volume on the NCL for p’= 1 kPa
λ	gradient of the NCL in the v-ln$_{p}$’ space
M	critical state stress ratio
p'_{cs}	equivalent pressure on the CSL
p_e^*	equivalent pressure on the INCL* of the reconstituted samples

1. Introduction

Embankment slope failure, due to desiccation cracks, stress relaxation and pore pressure increase is one of the major problems frequently encountered on the road networks around the world. The remediation works cause congestion and delays that, in turn, cause financial loss. Traditionally adopted chemical stabilisation methods such as lime, cement, ash and others, cause health problems and great environmental impact. To reduce maintenance costs associated with delays caused by the reinstatement of failed slopes, the use of fibres is proposed as a more sustainable and environmentally friendly approach.

It is textbook knowledge that soil reinforcement works for dilative soils (usually granular soils), and not conventionally considered effective for clays with low apparent friction angle. However due to the ease of application and reduced environmental impact, the use of fibres in cohesive soils is attracting interest of many researchers. Li and Zornberg (2019, 2013, 2003) reported that the fibre treatment substantially increase the peak shear strength and reduced the residual strength loss. Li (2005), Freilich et al. (2010) and Mirzababaei et al. (2017) evaluated the undrained shear behaviour of fibre-reinforced clay and reported that fibres restrict dilation, leading to an increase in the excess pore pressure. Authors attributed this observation to the fibres distributing stresses more uniformly within the soil matrix. Similar conclusions were reached by Ekinci and Ferreira (2012), Tang et al. (2007), Özkul and Baykal (2007), Freilich et al. (2010), Botero et al. (2015) and Yi et al. (2015) when investigating the deformation modes of different fine grained soils. All authors reported the development of distinct slip planes on unreinforced samples, while reinforced specimens showed a barrelling type failure. As an influence on such observed behaviour, Ekinci and Ferreira, (2012) and Diambra et al. (2007), studied the orientation of fibres after preparation of samples and reported that the vast majority of the fibres are aligned horizontally that contributes to change in failure mode from district slip plane to barrelling. In a more recent study Mirzababaei et. al. (2020) statistically quantified the re-orientation of fibres during shearing with the aid of X-Ray computed tomography imaging technique. In agreement with earlier studies, authors reported that most fibres, in a randomly fibre reinforced clays, will align near-horizontally once subjected to vertical loading. In addition, Maher and Gray (1990); Li and Zornberg (2005); Özkul and Baykal (2007), Dos Santos et al. (2010), Yi et al. (2015) and Anggraini et al. (2016) studied the effect of the confining pressure on the response of discrete fibre-reinforced soils under static loading, concluding that inclusion of fibres increases friction angle of fiber-reinforced soil at low confining pressures. When confining pressures increases beyond a 'critical' value, the friction angle of fiber reinforced soil becomes close to that of unreinforced soil, but the shear strength was still higher than that of unreinforced soil because of the increased apparent cohesion. Ayeldeen and Kitazume (2017); Jamsawang et al. (2018) and Tang et al. (2016) reported that fibre surface roughness is another important aspect that defines the mechanical performance of fibre reinforced soils. Li et al. (2005) and Valadez-Gonzalez et al. (1999) proposed fibre surface treatment methods to increase surface roughness and provide better mechanical interlocking and interfacial load transfer efficiency.

Silva Dos Santos et al. (2010) were among the few who performed high pressure laboratory studies on fibre-sand mixtures and adopted a critical state framework to describe its mechanical behaviour. Li et al. (2017) conducted dynamic and monotonic triaxial testing to study the behaviour of carbon fibre-reinforced recycled concrete aggregates by focusing on the very small and large strain ranges. Authors reported that, at large strains, reinforced and unreinforced specimens showed comparative stress-strain response and volumetric behaviour with very similar critical state parameters, with fibre reinforced specimens having slightly higher critical state angle of shear strength. More recently Fu et al. (2018) utilised critical state framework to compare the performance of polypropylene and rubber fibres in well-graded decomposed granite. In a similar study Madhusudhan et al. (2017) examined the effect of adding fibres to a completely decomposed granite (CDG) in light of critical state framework. Authors reported that while unreinforced CDG is sensitive to sample preparation, the reinforced soil is not sensitive to the method of material or sample preparation. In a more recent attempt Mirzababaei et al. (2018) performed consolidated undrained triaxial tests to study the shear strength of fibre-reinforced clays using waste carpet fibres and proposed a nonlinear regression model to predict the relationship between effective shear stress ratio, deviator stress, axial strain, and the fibre content. The developed model worked well to predict the shear strength of fibre-reinforced clays.

It is evidential from earlier studies that, until now, not many have attempted to highlight the influence of the fibre induced structure on cohesive soils, with respect to a well-established framework.

To determine the properties of compacted heavily overconsolidated clays samples are prepared using a traditional sample preparation method that: a) destructure completely the clay to achieve the required moisture content and b) reuse the soil. This may be adequate to normally and lightly overconsolidated clays but do not represent adequately the in-situ response of compacted soil. This becomes even more problematic when reinforcement is added to the soil. In this article, the effect of fibre reinforcement on the large strain behaviour of compacted clay samples, tested using large triaxial equipment is investigated. A novel specimen preparation method is proposed, where peds of clay are compacted to closely simulate the in-situ compaction procedure observed. A large number of 100 × 200 mm triaxial tests and one-dimensional compression tests were performed on compacted reinforced and unreinforced samples. The results have been discussed in three separate sections: the first section evaluates the effect of sample preparation and their proposed procedure (reconstituted versus unreinforced); the second section highlights the sole effect of fibres (unreinforced versus reinforced) and a final discussion section where the effect of the preparation methods and the addition of fibres were further examined. This paper also discusses the structural role of fibres during isotropic compression, and the 'metastable' nature of this structure once it yields upon shearing.

2. Materials

The soil used in this study was sampled from a site adjacent to the slip road onto the northbound carriageway of the A1(M) motorway, near the junction with the M25 motorway, in London, UK. The site consisted of a 5-m-high cut with a slope angle of approximately 15°, bounded at the top by a field and at the bottom by the slip road. The soil is described as soft-to-firm fissured greenish grey mottled yellowish brown and red over-consolidated clay, pertaining to the Undivided Reading Formation from the Lambeth Group Clays. In their extensive study of Lambeth group clays Hight et al. (2004) reported that a large amount of the formation comprises of largely unbedded, mottled silty clay and clay alone. Authors added that during the deposition of the Lambeth group, fissures with polished and slickensided surfaces have developed due to desiccation throughout seasonal changes in ground moisture.

Soil classification tests were performed in accordance with BS 1377-2:1990.The liquid and plastic limits of the clay were 72% and 33%, respectively. Grain size distribution analysis indicated that the clay size content was around 47%. According to USCS classification (ASTM 1993), the clay was classified as inorganic clay with high plasticity (CH). The average particle density (ρs) was 2.65 g/ml.

Polypropylene tape type fibres, 4 mm wide, 63 mm long and 0.021mm thick, supplied by Fibre Soils, were mixed at contents of 0.2% of the dry weight of soil. The physical, chemical, and mechanical properties of the fibres, provided by the manufacturer, are presented in Table 1.

3. Sample preparation procedure and testing program

3.1. Unreinforced reconstituted samples

Reconstituted samples were created from a slurry prepared at 1.25 times the liquid limit (Burland, 1990) and consolidated to a vertical effective stress of 88 kPa using a consolidometer. This was the lowest possible pressure to obtain a specimen with sufficient consistency for testing in the triaxial equipment. The samples were extracted from the consolidometer, trimmed to the desired height and diameter (76 x 38 mm) and transferred to the triaxial equipment where an isotropic effective stress of 40 kPa was applied and maintained during saturation with a 40 kPa back pressure. Since soil reconstitution erases the effect of structure, the test results obtained from these samples form a reference point to evaluate the effect of fibre reinforced and unreinforced ped compaction. All samples prepared via consolidometer were isotropically consolidated; normally consolidated samples allowed the determination of the Roscoe surface whilst samples REC-450-200 and REC-500-125 were over-consolidated to define the Hvorslev surface to determine the reconstituted state boundary surface (SBS*).

3.2. Unreinforced ped-compacted samples

On the area where the soil was collected, a failed slope was being reinstated using fibre reinforcement (Highways England approved departure from standards), when traditionally lime would be used. The procedure followed by the contractor can be seen on Fig. 1; to create reinforced layers, soil was spread over the required area with fibres manually spread on top. A rotovator was used to break the large soil lumps into 5-10 cm diameter pieces and mix the fibres in the mass, before compaction. This procedure created 20 cm thick compacted layers and was followed to top of the slope. It is not the scope of this paper to analyse the reinstated slope, however the simplified procedure described above is relevant because of the heavily overconsolidated nature of the Lambeth group clays. It is likely that the compacted soil retains some of the original clay structure but may not behave in the same way as the intact soil. By observing what happened in-situ, a new sample preparation technique was developed to closely simulate the structure created on site at the laboratory environment. This procedure was adapted from O'Connor (1994), after a model proposed by Brackley (1975) that considered that the unsaturated clay existed as packets of saturated soil particles and the inter-pocket voids were filled with air. By assuming that the packets were saturated, Brackley (1975) developed the idea that the individual pockets retain the properties of the natural soil and the total volume change of the soil mass is due to the sum of the effects of swelling or compression of the pockets of air and shear behaviour of the clay packets. Yong & Warkentin (1975) identified "peds" as fabric units that can be identified visually with the naked eye and consist of an finite aggregation of packets and pockets. In a more recent study on marine clays, Ekinci (2019) reported that, to some extent, peds retain the in-situ structure and produce strengths close to in-situ unconfined compressive strength.

During the preparation of unreinforced ped-compacted samples in the laboratory, the undisturbed soil was chopped into pieces of 10–15 mm in diameter (called peds) and stored in sealed barrels (Fig. 2). To achieve the desired moisture content (MC), the peds were either dried by leaving the barrel open and allowing the moisture to evaporate or moistened by spraying water on the ped surfaces. To ensure that the moisture was uniformly distributed within the peds, distilled water was sprayed at regular intervals over a period of 24 h, while the barrel was rolled on the ground to mix the aggregates and help the exchange of moisture. During this process, samples from three different locations in the barrel were collected and their MC determined. Care was taken to keep the difference in MC contents at various positions below 0.5%. An initial triaxial test on a sample compacted at the optimum moisture content (OMC) proved extremely difficult to saturate, therefore, to help with the saturation, all samples were compacted near the saturation line, or 2% wet of the optimum, according to the compaction curve determined previously (Ekinci and Ferreira 2012). The compaction tests showed that the fibres had a small effect on OMC and the maximum dry density (MDD) of the soil: 21.5% and 1.68 g/cm^3 for the compacted soil with fibres, and 20.5% and 1.70 g/cm^3 for the compacted samples without fibres.

Once the MC of the peds was considered homogeneous, they were compacted in a 100 mm diameter and 200 mm in height, using light compaction (BS 1377-4:1990), where the sample was built in 5 layers with 25 blows per layer. After compaction, samples were trimmed down to 38 mm in diameter and 76 mm in height. Testing small samples was necessary in order to drastically reduce the duration of the tests. Specimens prepared under the same conditions have been tested on triaxial equipment and confirmed that there is no effect of specimen size on the mechanical response of the prepared samples (Ekinci, 2016).

3.3. Fibre reinforced ped-compacted samples

The fibre reinforced ped-compacted samples were prepares in a similar way as unreinforced ped-compacted samples. Only difference in the process was the fibre addition part. Fibres were added by mixing, in a sealed zip-lock bag the necessary weight in clay peds and fibres. To avoid fibre agglomeration, considerable care was taken to mix the peds and the fibres by revolving the zip-lock bag in all directions for approximately 5 min or until a visually uniformity was achieve.

Furthermore, during triaxial testing all tested specimens were saturated until a B-value above 95% was reached. Table 2 shows a summary of all triaxial tests and define the sample names used in the paper.

3.4. Oedometer samples

Oedometer samples of reinforced and unreinforced ped-compacted specimens with 75 mm diameter were prepared in a similar way as triaxial samples; the soil was compacted into a compaction mould that contained the oedometer ring inside, maintaining a similar compaction energy. The oedometer ring was placed at the bottom of the first layer and the soil was carefully inserted without moving the ring from its central position. Afterwards, the sample was extruded from the mould and trimmed for testing. In order to test the reinforced samples, an oedometer ring with 40 mm in height was used to accommodate the fibres. Table 3 shows a summary of all oedometer tests and define the sample names used in the paper.

The void ratio of all tested specimens were calculated using four methods, considering the initial and final moisture content, along with the initial bulk and dry unit weights and the specific gravity of the fibres; the average value for each sample is reported. Despite the careful preparation and measurement of MC, variations in the initial MC of the compacted samples resulted in uncertainties in the initial void ratio of ±0.01–0.02.

4. Effect of sample preparation via ped compaction

Fig. 3 shows the paths followed during the isotropic compression of the unreinforced reconstituted and ped-compacted samples on the v versus log p' space. The REC500 and REC 450_200 reconstituted specimens that have consolidated to high stresses have followed a unique intrinsic normal compression line (INCL*), characterised by equation 1, where N=2.51 and λ=0.165. It is not possible to estimate a distinct isotropic normal compression line (iso-NCL) for the unreinforced ped-compacted specimens, where even at high stresses the compression lines seem to stay parallel and do not reach a single NCL. The gradient of the compression lines of the unreinforced ped-compacted samples was calculated as λ=0.092, by using equation 2, the value of Cc can be transferred to the v versus lnp' space and the value determined is 0.095, similar to the value of 0.092 determined later from one-dimensional compression of unreinforced ped-compacted specimens.

$$v = N - \lambda lnp' \qquad (1)$$

$$\lambda = \frac{Cc}{2.303} \qquad (2)$$

The unreinforced ped-compacted specimens showed an extensive yielding zone, where yielding occurred on much higher stresses than reconstituted samples, closer to the INCL*. The gradient of the iso-NCL of both specimens was smaller than that of the INCL*. This response is similar to the behaviour reported by Vitone and Cotecchia (2011) for scaly clays and Hight et al. (2007) for natural London Clay and was possibly dependent on the sample preparation. It can be initially thought that due to the sample preparation method, where natural samples are chopped into 10 to 15 mm peds, the fissures were destroyed. However, due to the compaction technique and the presence of peds, it was monitored that the peds deformed and filled the gaps between other peds, creating a heterogeneous structure similar to a randomly fissured sample.

The stress–strain relationships of the reconstituted and ped-compacted unreinforced specimens are compared in Fig. 4a. Two reconstituted samples were over-consolidated (ratios of 4 and 2) to allow the definition of the full SBS*. The unreinforced ped-compacted samples sustained much higher deviatoric stresses for all confining pressures, particularly since the samples were created by compaction of peds; these are likely to be due to the compaction effort and lower initial void ratios, allowing the soil to reach higher shear strengths.

In Fig. 4b, unreinforced reconstituted and ped-compacted samples with the same confining pressures, e.g. 150 and 500 kPa, experienced identical increases in excess pore pressures up to 2% strain. At higher strains, stabilisation or reduction in pore pressure was observed for the unreinforced ped-compacted soils, whilst the reconstituted sample either stabilised or showed a slight increase in pore pressure. The over-consolidated samples showed a similar response to the unreinforced ped-compacted samples, where similar pore pressures were measured at similar confining stresses.

To understand the pore pressure responses, the failure mechanism of the samples after shearing was analysed. The barrelling failure mode of the reconstituted specimens resulted in homogeneous pore pressure distribution throughout the sample, indicated by the constant change in pore pressure from medium- to high-strain levels. In the unreinforced ped-compacted specimens, strain localisation was observed in some samples, causing excess water to drain towards the shear plane, reducing the global pore pressure in the sample. Furthermore, a reduction in the deviatoric stress due to an increase in pore pressure was observed for the samples tested at high confinements.

The increase in the pore pressure of the reconstituted specimens was more pronounced for specimens tested at high confinement stresses (500 kPa), resulting in a reduction in the effective stresses acting on the soil, causing the stress path to bend to the left, producing lower shear strength. This behaviour was observed for the curves shown in Fig. 5 for the reconstituted and ped-compacted unreinforced specimens. In addition, the critical state stress ratio (M) values of the reconstituted samples (0.85) were lower than that of the unreinforced ped-compacted samples (0.89).

Fig. 6 shows the results of the consolidation stage, together with data points from the end of the triaxial tests, or, in the case of the reconstituted samples, when the samples reached a critical state. The arrows indicate the path the samples were following at the end of the test, when a critical state was not reached. The least complete tests are of samples with the lowest confining stresses (REC-150 and REC-500-125), which were still experiencing further increases in stress and reduction in pore water pressure. Samples REC-500 and REC-450-200 reached a critical state indicated by a constant shear strength and constant excess pore pressure. In addition, a single drained test was performed with a reconstituted sample (D-REC-150), where the end of the test defined a CSL parallel to the previously determined NCL, with parameters of λ = 0.165 and Γ = 2.498. Furthermore, the INCL* of this reconstituted soil seams to be parallel to the INCL* of London clay.

Fig. 7 shows v vs. lnp' plots for the unreinforced ped-compacted samples during isotropic consolidation and the last points from the triaxial tests. The results of the unreinforced ped-compacted specimens seem to show that the CSL is not unique but proportional to the initial void ratio of the samples tested as shown previously by Ferreira and Bica (2006) and Ponzoni et al. (2014). Since there seems to be a multiple number of parallel NCLs, which depended on the initial void ratio of the specimens, two CSLs were introduced, similar to that proposed by Ferreira and Bica (2006).

Samples U-NF-150, 300, and 500 are clearly on the CSL_1. For sample U-NF-100, the stresses were not stable, but the test seemed to be moving towards a CSL_1. Samples U-NF-50, D-NF-100, and D-NF-300 were on the wet side of the CSL_1 and were moving away from the CSL_1. Therefore CSL_2 was introduced that has the same slope as CSL_1 and the NCLs. The slopes of the iso-NCLs for the unreinforced ped-compacted specimens were determined according to the isotropic compression behaviour discussed earlier (Figure 3), where the parameters defining the CSL_1 and CSL_2 for the unreinforced soil are λ = 0.092, Γ_1 = 2.071, and Γ_2 = 2.157. It is important to note that the excess porewater generation trends (Fig 4b) of two different types of specimens (reconstituted and ped-compacted) would work as an attractor during shearing and influences the location of the CSL in the v-lnp` plane.

5. Effect of discrete fibre incorporation

The effect of discrete fibre addition has been assessed in one dimensional compression by testing unreinforced ped-compacted samples to determine a reference behaviour that will be used to understand the effects of reinforcement in one-dimensional compression (Table 3). As can be seen on Fig. 8, both reinforced and unreinforced ped-compacted samples are not following identical compression lines. Unreinforced samples seem to reach a set of parallel lines, that are dependent of the initial void ratio, whilst the reinforced samples seem to continue and converge to an area where an NCL could be defined. It is also important to mention that the current stress levels are not enough to reach a unique NCL, particularly in the case of the unreinforced specimens, where an NCL could be reached at void ratios as low as 0.30, where the NCL would start becoming flatter.

Ponzoni et al., (2014) introduced the parameter “m” to provide a convenient way of quantifying the degree of convergence and perhaps the transitional behaviour degree. Authors reported that for soils that converge to a unique NCL m = 0, whilst for soils with perfectly parallel compression paths m = 1. Figure 9 was used to quantify the degree of convergence of the data on Fig.8, the initial specific volumes determined at 20kPa vertical stress (V_{20}) were plotted against the final specific volume at 1400kPa (V_{1400}), the maximum stress reached in the tests. The gradient of the best fit line through the points defines the “m” parameter. Fig. 9 confirms the difficulty to define a unique NCL for the unreinforced, as indicated by the value m=0.96. However, for the reinforced soil, the value m=0.14 indicate that a unique NCL can be determined.

Further comparison of the triaxial test results for reinforced and unreinforced ped-compacted soils provided insight into the effect of fibre addition on the mechanical behaviour and failure mechanism of the samples. As shown in Fig. 10a, all reinforced ped-compacted samples showed strain-hardening behaviour for medium-to-high strain levels, while the unreinforced ped-compacted samples tested at a confining stress of 150 kPa showed a small peak and a small reduction in deviatoric stress at strains >14%. Similar behaviour was observed by Özkul and Baykal (2007), where this difference was attributed to the effect of fibres stretching across the shearing area and restricting the development of a slip plane by transferring shear stress and strains over wider areas. This behaviour was also similar to that observed by Maher and Gray (1990), Li and Zornberg (2005), and Mirzababaei et al. (2018). At lower confining stresses (<100 kPa), the reinforced ped-compacted samples reached higher deviatoric stresses than the unreinforced ped-compacted samples.

The pore water pressure generated by the reinforced ped-compacted samples during shearing was consistently higher than that of the unreinforced ped-compacted samples (Fig. 10b) due to the effect of the fibres on sample deformation. Li (2005) and Freilich et al. (2010) reported that this is due to the fibres distributing stresses within the soil mass and increasing the contractive deformations within the fibre-soil matrix. Reinforced ped-compacted soils tend not to contract significantly during consolidation, however, generate higher pore pressures when sheared due to their higher volume reductions compared to unreinforced ped-compacted samples. It would thus appear that the fibre reinforcement provides a form of macrostructure during compression that allows it to attain volumetric state conditions that are impossible for the unreinforced soil. However, this macrostructure is metastable due to the contractive response during shearing. This phenomenon also allowed the fibres to transfer stresses over wider areas within the sample, compared to the pure clay; even at 20% strain no single shear plane was observed for the reinforced ped-compacted specimens. However, the unreinforced ped-compacted samples showed a distinct shear plane for strains >5% (Ekinci and Ferreira, 2012). Both Table 2 and the volumetric response graphs showed that these effects occurred regardless of the confinement stress or pre-shear volumetric state. Visually, the results obtained here are similar to those obtained by Freilich et al. (2010) and Özkul and Baykal (2007).

The failure mechanisms agree with the pore water pressure distribution of the samples. In unreinforced ped-compacted samples, at strains around which the shear plane was formed, the pore water pressures started to drop slightly as the water drains towards the shear zone. Atkinson and Richardson (1987) reported that flow of water towards the shear zone forms local drainage conditions and influence measurements of undrained shear strength. For the reinforced ped-compacted samples, a shear plane was not formed due to the tensile strength provided by the fibres, which was in agreement with the results of measurements performed with the mid-height probe and the MC data taken from five different height locations within the specimens after shearing.

Fig. 11a shows the results of constant p’ drained tests performed on samples of reinforced and unreinforced ped-compacted soil, where the unreinforced ped-compacted samples showed a slight peak and subsequent decrease where the reinforced ped-compacted ones showed strain hardening behaviour. It is not possible to identify any notable strength difference between fibre reinforced and unreinforced ped-compacted samples as the observed difference is within the expected experimental variability. Volumetric strain response of fibre reinforced and unreinforced ped-compacted samples under drained conditions are shown in Fig. 11b. The reinforced and unreinforced samples ped-compacted showed different volumetric changes under shearing. The rate of dilation of the reinforced ped-compacted samples was consistently higher than the unreinforced ped-compacted samples. At the end of the tests, the net volumetric strain was negative for all samples, where the reinforced samples showed greater dilation than the unreinforced samples for similar effective stresses.

The representative drawing of the failure modes of each tested specimens can be seen on Fig. 12. These were drawn based on measurements taken at the end of each drained test. It is clear that the reinforced ped-compacted specimens show a barrelling failure, whilst the unreinforced ped-compacted have failed with formation of a shear plane. Reinforced samples were aided by the near-horizontal aligned fibres due to compaction (Ekinci and Ferreira 2012) where the fibres help to bridge the shear plane and result in localised shear bands rather than a large single shear surface.

Stress paths of reinforced and unreinforced ped-compacted specimens together with their failure envelopes can be seen on Fig. 13. It can be seen that reinforced ped-compacted specimens tested at high confinement observed to have reduction in the effective stresses acting on the soil, causing the stress path to bend to the left, leading to a lower shear strength. It is worth to mention that U-NF-500-300 sample (plotted behind D-NF-300 in Fig. 13) tend to develop less excess pore pressure when compared to U-NF-300 and reaches lower deviatoric stresses due to over consolidation effect. This is expected effect of over-consolidation as increase in OCR courses increase in deviatoric stress and reduction in excess pore water pressure development (Gu et. al. 2016). In addition, the critical state stress ratio (*M*) values of the reinforced samples (0.87) were slightly lower than that of the unreinforced samples (0.89).

Furthermore, Fig. 14 shows the end of test points of the ped-compacted samples with fibres. Specimens D-F-100, U-F-300 and U-F-500 reached a well-defined CSLs with parameters of λ = 0.061 and Γ = 1.893 (i.e., a much lower slope than that of the unreinforced soil). The testing of sample U-F-150 finished near the CSL, whilst samples D-F-50 and U-F-100 finished far from the determined CSL. Nevertheless, unlike unreinforced specimens, reinforced specimens which are not on the CSL are showing a tendency to reach a single critical state line whilst D-F-50 is contracting towards the CSL.

6. Further insight on the mechanics of the ped compaction and fibre inclusion

All the NCLs and CSLs determined for the different soil samples are plotted in Fig. 15, together with the compression lines for reconstituted and natural London clay (Gasparre 2005). The INCL* of this reconstituted soil was parallel to the INCL* of London clay. As discussed earlier these soils belong to adjacent geological units and having similar characteristics. Therefore, it is not a coincidence that they have parallel INCL*s. The figure also shows that the London clay iso-NCL (Gasparre 2005) had a similar slope to the ped-compacted unreinforced specimens tested in this study. All normal compression and critical state parameters determined from Fig. 15 are shown in Table 4. According to authors such as Silva Dos Santos et al. (2010), the critical state line (CSL) of the reinforced material coincided with the critical state line (CSL) of the unreinforced material at larger stresses, however the results obtained here are clear when they show that a constant strength state has been achieved in the triaxial equipment.

One can argue that the M values of the samples were close to each other, therefore it is not clear whether or not there is an influence of the addition of fibres or the ped-compaction (preparation). Moreover, to highlights the influence of the fibres and the ped-compaction induced structure on the soil, all tests were normalised by the equivalent pressure on the intrinsic normal compression line of the reconstituted samples (p_e*), given that the reconstituted soil showed a unique NCL with $\lambda = 0.165$ and $N = 2.51$. The value of p_e* was calculated using equation 3 below.

$$p`_e = exp[(N - v)/\lambda] \quad (3)$$

Fig. 16 presents the SBS* of the reconstituted soil and the normalised stress paths of the unreinforced and reinforced ped-compacted samples. It was possible to determine a unique SBS* with the CSL located at its apex. Since only undrained tests were used to determine this boundary, it is likely that it is a local boundary surface (LBS); according to Gens (1982) and Jardine et al. (2004) the LBS is a boundary surface that exists within the more extensive State Boundary Surface (SBS), which provides the outermost boundary between permissible and non-permissible normalised effective stress states. Zdravković and Jardine (2001) stated that if the plasticity of the reconstituted material is considered, the true SBS* is not expected to plot far above this LBS. Therefore, the LBS identified here will be treated as the Roscoe-Rendulic surface of the reconstituted set of tests. Additionally, only the dry side of the boundary surface of the reinforced and unreinforced ped-compacted specimens were drawn as it was not possible to consolidate the samples to stresses that would bring the compacted samples to the NCL and define the Roscoe-Rendulic surface.

Starting from the low pressures, the boundary surface of the unreinforced ped-compacted specimens extended well above the SBS*, clearly indicating the effect of the existing structure created by the compaction of the peds. It is worth mentioning that the intact and reconstituted (intrinsic) London clay SBS presented by the peak states of the clay from different units plot significantly above the state boundary surface from the reconstituted specimens (SBS*) for isotropically consolidated samples; this was considered a feature of the natural structure of the clay by Gasparre et al. (2007). It can be seen on Fig. 16 that the reconstituted Lambeth group clays SBS is identical to the reconstituted London clay SBS. Similar conclusion can be achieved when comparing the intact London clay SBS with the SBS defined by the unreinforced ped-compacted specimens. Although this may be a coincidence, it could also indicate that the peds present in the unreinforced ped-compacted samples retained part of their structure, even after compaction, to warrant a difference between SBS* and SBS similar to the one found in London clay. This is thought to be reasonable considering that both soil groups have a similar geological history.

Furthermore, the presence of fibres in the ped-compacted specimens produced an SBS slightly smaller than that of the unreinforced ped-compacted samples. It appears that the compaction of peds of reinforced samples introduced a fissure pattern created during compaction of peds plus fibres. Hight et al. (2007) reported a similar phenomena that there are two state boundaries in London clay where the upper bound is defined by the peak failure envelope of the intact clay without fissures, while the lower bound is given by the parameters defining the strength of the fissures. On a study with similar highly fissured and structured clay, Vitone and Cotecchia (2011) reported that the SBS of the un-fissured clay is larger than that of the reconstituted clay, while the SBS of a clay with a high fissure intensity is smaller than the same reconstituted clay. The authors further suggested that the intense fissuring degrades the mechanical properties of the clay, with respect to both the original unfissured material and the reconstituted soil.

Evaluation of the boundary surfaces in Fig. 16 also reveal a tendency to follow a parallel set of NCLs, even though the initial densities of the samples were different. When transitional behaviour is observed in dense clay specimens, normalising with respect to INCL* can be used to evaluating the effects of structure. Therefore, it can be summarised that the SBS is smaller due to the looser-than-possible (quasi-structure permitted, after Leroueil and Vaughan, (1990) regarding weak rocks) volumetric states resulting from the fibre reinforcement, but the yield surface is certainly larger for the same reason.

7. Conclusions

From the results presented in this study, the following conclusions can be drawn:

- Fibre reinforcement resulted in larger pore pressure developments in undrained testing and relatively small gains in performance during drained testing with slight increments in dilation rate.
- Fibre reinforcement prevents the single-slip plane strain localisation observed in unreinforced ped-compacted specimens but might have produced metastable contacts between peds.
- It is not possible to estimate a distinct NCL for the reinforced and unreinforced ped-compacted clays. The unreinforced specimens followed different, but parallel, compression lines for each initial void ratio, while the reinforced specimens converged to a unique NCL, making the determination of *Cc* difficult. This was attributed to the induced heterogeneity cause by the compaction method leading to a transitional behaviour.
- The CSL was not unique for the reinforced and unreinforced ped-compacted specimens, but proportional to the initial void ratio of the samples. Hence, there was strong evidence that the sample preparation method generated a transitional material. However, it was clear that the addition of reinforcement drastically reduced the transitional behaviour of samples tested under both compression and shear.
- Normalisation of all specimens using INCL* seams to effectively highlight the structural role of fibres during isotropic compression, and the 'metastable' nature of this structure once it yield upon shearing. It was possible to determine an SBS* for the reconstituted samples, but not for the reinforced and unreinforced ped-compacted soils due to stresses higher than the engineering stresses being required.
- Observation of the boundary surfaces of the ped-compacted reinforced samples laid below ped-compacted unreinforced specimens, is characteristic of fissured clays.

Furthermore, the compaction of peds of reinforced samples introduced a fissure pattern, where the fibres further introduce more intense fissuring created during compaction of peds and fibres.

- It is recommended that a similar study be conducted by evaluating the in-situ undisturbed natural samples of Lambert group and undisturbed fibre reinforced in-situ ped-compacted specimens to concrete the hypothesis that peds are retaining the structure of the natural specimen and further mimics the site compaction method respectively.
- Furthermore, the reduced boundary surfaces of fibre reinforced ped-compacted samples might be due to presence of the fibres introducing slickenside-like surfaces. Nevertheless, such hypotheses should be carefully substantiated by experimental observation and data.

Acknowledgements

The authors would like to thank the UK Engineering and Physical Sciences Research Council (EPSRC); Mouchel (Kier Group PLC) for their invaluable support during this research and Highways Agency (Highways England) for facilitating access to the site and support the research.

Funding

The authors express their appreciation to UK Engineering and Physical Sciences Research Council (EPSRC) for funding this research group. Scientific Research Project Reference EP/G011680/1.

Conflicts of interest/Competing interests

I confirm that this manuscript has not been published elsewhere and is not under consideration in whole or in part by another journal. The authors have no conflicts of interest to declare.

Data Availability Statement

Some or all data, models, or code that support the findings of this study are available from the corresponding author upon reasonable request.

Code availability

Not applicable

Authors' contributions

A. Ekinci has prepared the draft copy of the manuscript, conducted the PhD research study and manage the field works, M. Rezaeian has conducted some parts of analysis and formatting the manuscript, P. Ferreira was awarded the grant as a PI and supervised the research; he also wrote the discussion and parts of the introduction section, reviewing and editing the complete original copy of the manuscript.

References

Anggraini, V., Asadi, A., Farzadnia, N., Jahangirian, H., Huat, B.B.K., 2016. Effects of coir fibres modified with Ca(OH)2 and Mg(OH)2 nanoparticles on mechanical properties of lime-treated marine clay. Geosynthetics International 23(3): 206-218. doi: 10.1680/jgein.15.00046

ASTM D 2487-93, 1993. Standard classification of soils for engineering purposes. ASTM, Philadelphia, USA.

Atkinson, J.H., Richardson, D., 1987. The effect of local drainage in shear zones on the undrained strength of overconsolidated clay. Géotechnique, 37(3): 393–403. doi: 10.1680/geot.1987.37.3.393.

Ayeldeen, M., Kitazume, M., 2017. Using fiber and liquid polymer to improve the behaviour of cement-stabilized soft clay. Geotextiles and Geomembranes, 45(6), 592-602. doi: 10.1016/j.geotexmem.2017.05.005

Botero, E., Ossa, A., Sherwell, G., Ovando-Shelley, E., 2015. Stress-strain behavior of a silty soil reinforced with polyethylene terephthalate (PET). Geotextiles and Geomembranes, 43(4), 363-369. doi: 10.1016/j.geotexmem.2015.04.003

Brackley, I.J.A., 1975. The interrelationship of the factors affecting heave of an expansive, unsaturated clay soil. PhD thesis, University of Natal, Natal.

British Standard Institution, 1990. Methods of test for soils for civil engineering purposes. BS 1377, British Standard Institution, London

Burland, J.B., 1990. On the compressibility and shear strength of natural clays. Géotechnique, 40(3): 329-378.

Burland, J.B., Rampello, S., Georgiannou, V.N., Calabresi, G., 1996. A laboratory study of the strength of four stiff clays. Géotechnique, 47(2): 390–390. doi: 10.1680/geot.1997.47.2.390.

Diambra, A., Russell, A.R., Ibraim, E., Muir Wood, D., 2007. Determination of fibre orientation distribution in reinforced sands. Géotechnique, 57(7): 623–628. doi: 10.1680/geot.2007.57.7.623.

Ekinci, A., 2019. Effect of preparation methods on strength and microstructural properties of cemented marine clay. Construction & Building Materials, 227(116690)

Ekinci, A., 2016. The mechanical properties of compacted clay from the Lambeth group using fibre reinforcement. PhD thesis, University College London, London.

Ekinci, A., Ferreira, P.M.V., 2012. The undrained mechanical behaviour of a fibre-reinforced heavily over-consolidated clay, in ISSMGE - TC 211 International Symposium on Ground Improvement, Brussels, Belgium.

Ferreira, P.M.V., Bica, A.V.D., 2006. Problems in identifying the effects of structure and critical state in a soil with a transitional behaviour. Géotechnique, 56(7): 445-454.

Freilich, B., Li, C., Zornberg, G., 2010. Effective shear strength of fiber-reinforced clays, in 9th International Conference on Geosynthetics, (Icd), pp. 1997–2000.

Fu, R., Baudet, B.A., Madhusudhan, B.N. Coop, M.R., 2018. A comparison of the performances of polypropylene and rubber fibers in completely decomposed granite. Geotextiles and Geomembranes, 46(1), 22-28. doi: 10.1016/j.geotexmem.2017.09.004

Gasparre, A., 2005. Advanced laboratory characterisation of London clay. PhD thesis, Imperial College London, London.

Gasparre, A., Hight, D.W., Nishimura, S., Minh, N.A., Jardine, R.J., Coop, M.R., 2007. The influence of structure on the behaviour of London Clay. Géotechnique, 57(1): 19–31. doi: 10.1680/geot.2007.57.1.19.

Gens, A., 1982. Stress-strain and strength characteristics of a low plasticity clay. University of London

Gu, C., Wang, J., Cai, Y., Sun, L., Wang, P., Dong, Q., 2016. Deformation characteristics of overconsolidated clay sheared under constant and variable confining pressure. Soils and Foundations, 56(3): 427-439.

Hight, D.W., Ellison, R.A., Page, D.P., 2004. Engineering in the Lambeth Group. London: Ciria.

Hight, D.W., Gasparre, A., Nishimura, S., Minh, N.A., Jardine, R.J., Coop, M.R., 2007. Characteristics of the London clay from the Terminal 5 site at Heathrow Airport. Géotechnique, 57(1): 3–18. doi: 10.1680/geot.2007.57.1.3.

Jamsawang, P., Suansomjeen, T., Sukontasukkul, P., Jongpradist, P., Bergado, D.T., 2018. Comparative flexural performance of compacted cement-fiber-sand. Geotextiles and Geomembranes, 46(4), 414-425. doi: 10.1016/j.geotexmem.2018.03.008

Jardine, R. J., Gens, A., Hight, D. W., Coop, M. R. 2004. Developments in understanding soil behaviour. In Advances in geotechnical engineering: The Skempton conference: Proceedings of a three day conference on advances in geotechnical engineering, organised by the Institution of Civil Engineers and held at the Royal Geographical Society, London, UK, on 29–31 March 2004 (pp. 103-206). Thomas Telford Publishing.

Leroueil, S., Vaughan, P.R., 1990. The general and congruent effects of structure weak rocks. Géotechnique, 40(3): 467–488.

Li, C., 2005. Mechanical response of fiber-reinforced soil. PhD thesis, University of Texas at Austin, Austin.

Li, C., Zornberg, J., 2005. Interface shear strength in fiber-reinforced soil, in Proceedings of 16th International Conference on Soil Mechanics and Geotechnical Engineering. Osaka, Japan: 1373–1376.

Li, C., Zornberg, J.G., 2003. Validation of discrete framework for fiber reinforcement. in Proceedings of the 2003 North American Conference on Geosynthetics. Winnipeg, Canada: 285–293.

Li, C., Zornberg, J.G., 2013. Mobilization of reinforcement forces in fiber-reinforced soil. Journal of Geotechnical and Geoenvironmental Engineering, 139(1), 107-115. doi: 10.1061/(ASCE)GT.1943-5606.0000745

Li, C., Zornberg, J.G., 2019. Shear Strength Behavior of Soils Reinforced with Weak Fibers. Journal of Geotechnical and Geoenvironmental Engineering, 145(9), 2–8. doi: 10.1061/(ASCE)GT.1943-5606.0002109

Li, M., He, H., Senetakis, K., 2017. Behavior of carbon fiber-reinforced recycled concrete aggregate. Geosynthetics International, 24(5), 480-490. doi: 10.1680/jgein.17.00016

Li, Y., Mai, Y.W., Ye, L., 2005. Effects of fibre surface treatment on fracture-mechanical properties of sisal-fibre composites. Composite Interfaces, 12(1-2), 141-163. doi: 10.1163/1568554053542151

Madhusudhan, B. N., Baudet, B. A., Ferreira, P. M. V., & Sammonds, P., 2017. Performance of fiber reinforcement in completely decomposed granite. Journal of Geotechnical and Geoenvironmental Engineering, 143(8): 1-11

Maher, M.H., Gray, D.H., 1990. Static response of sands reinforced with randomly distributed fibers. Journal of Geotechnical Engineering, 116(11): 1661-1677.

Marsland, A., 1971. The shear strength of stiff fissured clays, in Proceedings of the Roscoe Memorial Symposium. Cambridge, UK: 59–68.

Mirzababaei, M., Arulrajah, A., Horpibulsuk, S., Aldava, M., 2017. Shear strength of a fibre-reinforced clay at large shear displacement when subjected to different stress histories. Geotextiles and Geomembranes, 45(5), 422-429. doi: 10.1016/j.geotexmem.2017.06.002

Mirzababaei, M., Mohamed, M., Arulrajah, A., Horpibulsuk, S., Anggraini, V., 2018. Practical approach to predict the shear strength of fibre-reinforced clay. Geosynthetics International, 25(1): 50–66. doi: 10.1680/jgein.17.00033.

Mirzababaei, M., Anggraini, V., Haque, A., 2020. X-ray computed tomography imaging of fibre-reinforced clay subjected to triaxial loading. Geosynthetics International, 27(6): 635-645.

O`Connor, A., 1994. Swelling Behaviour of Unsaturated Fine Grained Soils. PhD thesis, City University of London.

Özkul, Z.H., Baykal, G., 2007. Shear behavior of compacted rubber fiber-clay composite in drained and undrained loading. Journal of Geotechnical and Geoenvironmental Engineering, 133(7): 767–781. doi: 10.1061/(ASCE)1090-0241(2007)133:7(767).

Ponzoni, E., Nocilla, A., Coop, M.R., Colleselli, F., 2014. Identification and quantification of transitional modes of behaviour in sediments of Venice lagoon. Géotechnique, 64(9): 694–708. doi: 10.1680/geot.13.P.166.

Silva Dos Santos, A.P., Consoli, N.C., Baudet, B.A., 2010. The mechanics of fibre-reinforced sand Géotechnique, 60(10): 791–799. doi: 10.1680/geot.8.P.159.

Skempton, A.W., Petley, D.J., 1967. The strength along structural discontinuities in stiff clays, in Proceedings of the Geotechnical Conference. Oslo, Norway, pp: 29–45.

Skempton, A.W., Petley, D.J., Schuster, R.L., 1969. Joints and fissures in the London clay at Wraysbury and Edgware. Géotechnique, 19(2): 205–217. doi: 10.1680/geot.1969.19.2.205.

Tang, C., Shi, B., Gao, W., Chen, F., Cai, Y., 2007. Strength and mechanical behavior of short polypropylene fiber reinforced and cement stabilized clayey soil. Geotextiles and Geomembranes, 25(3): 194–202. doi: 10.1016/j.geotexmem.2006.11.002.

Tang, C.S., Li, J., Wang, D.Y., Shi, B., 2016. Investigation on the interfacial mechanical behavior of wave-shaped fiber reinforced soil by pullout test. Geotextiles and Geomembranes, 44(6), 872-883. doi: 10.1016/j.geotexmem.2016.05.001

Valadez-Gonzalez, A., Cervantes-Uc, J.M., Olayo, R., Herrera-Franco, P.J., 1999. Effect of fiber surface treatment on the fiber-matrix bond strength of natural fiber reinforced composites. Composites Part B: Engineering, 30(3), 309-320. doi: 10.1016/S1359-8368(98)00054-7.

Vitone, C., Cotecchia, F., 2011. The influence of intense fissuring on the mechanical behaviour of clays. Géotechnique, 61(12): 1003–1018. doi: 10.1680/geot.9.P.005.

Yi, X.W., Ma, G.W., Fourie, A., 2015. Compressive behaviour of fibre-reinforced cemented paste backfill. Geotextiles and Geomembranes, 43(3), 207-215. doi: 10.1016/j.geotexmem.2015.03.003.

Yong, R.N. & Warkentin, B.P., 1975. Soil Properties and Behaviour, Amsterdam: Elsevier Scientific Publishing Company.

Zdravković, L., Jardine, R.J., 2001. The effect on anisotropy of rotating the principal stress axes during consolidation. Géotechnique 51(1): 69–83. doi: 10.1680/geot.2001.51.1.69.

Figure Captions

Fig. 1. Steps followed during slope treatment with fibre reinforcement.

Fig. 2. Photographs of chopped clay peds in the storage drum and the polypropylene fibres used for reinforcement.

Fig. 3. Isotropic compression paths for the reconstituted and unreinforced specimens.

Fig. 4. (a) Stress–strain and (b) pore pressure response of unreinforced and reconstituted clay samples.

Fig. 5. Stress paths of unreinforced, and reconstituted clay samples.

Fig. 6. End-of-test states for the reconstituted samples.

Fig. 7. End-of-test states for the drained and undrained unreinforced samples.

Fig. 8. One-dimensional compression data for fibre reinforced and unreinforced samples.

Fig. 9. Calculation of m values for reinforced and un-reinforced specimens.

Fig. 10. (a) Stress-strain and (b) pore pressure response of reinforced and unreinforced clay samples.

Fig. 11. (a) Stress-strain and (b) change in volumetric strain response of Lambeth Group clay and fibre-reinforced clay samples under drained conditions.

Fig. 12. Shear plane characteristics for consolidated drained triaxial test of reinforced and unreinforced specimens.

Fig. 13. Stress paths of unreinforced and reinforced clay samples.

Fig. 14. End-of-test states for the drained and undrained reinforced samples.

Fig. 15. Determined CSLs and NCLs of all tested samples.

Fig. 16. State boundary surfaces of all specimens normalised by iNCL*, along with data from(Gasparre, 2005) for reconstituted and intact Unit A3 and B2&C clays.

Table Captions

Table 1. Properties of fibres

Table 2. Summary of all triaxial tests

Table 3. Specifications of 1-D Compression tests carried out for proposed study

Table 4. CSL and NCL parameters for the lines on Fig. 15

Figure 1

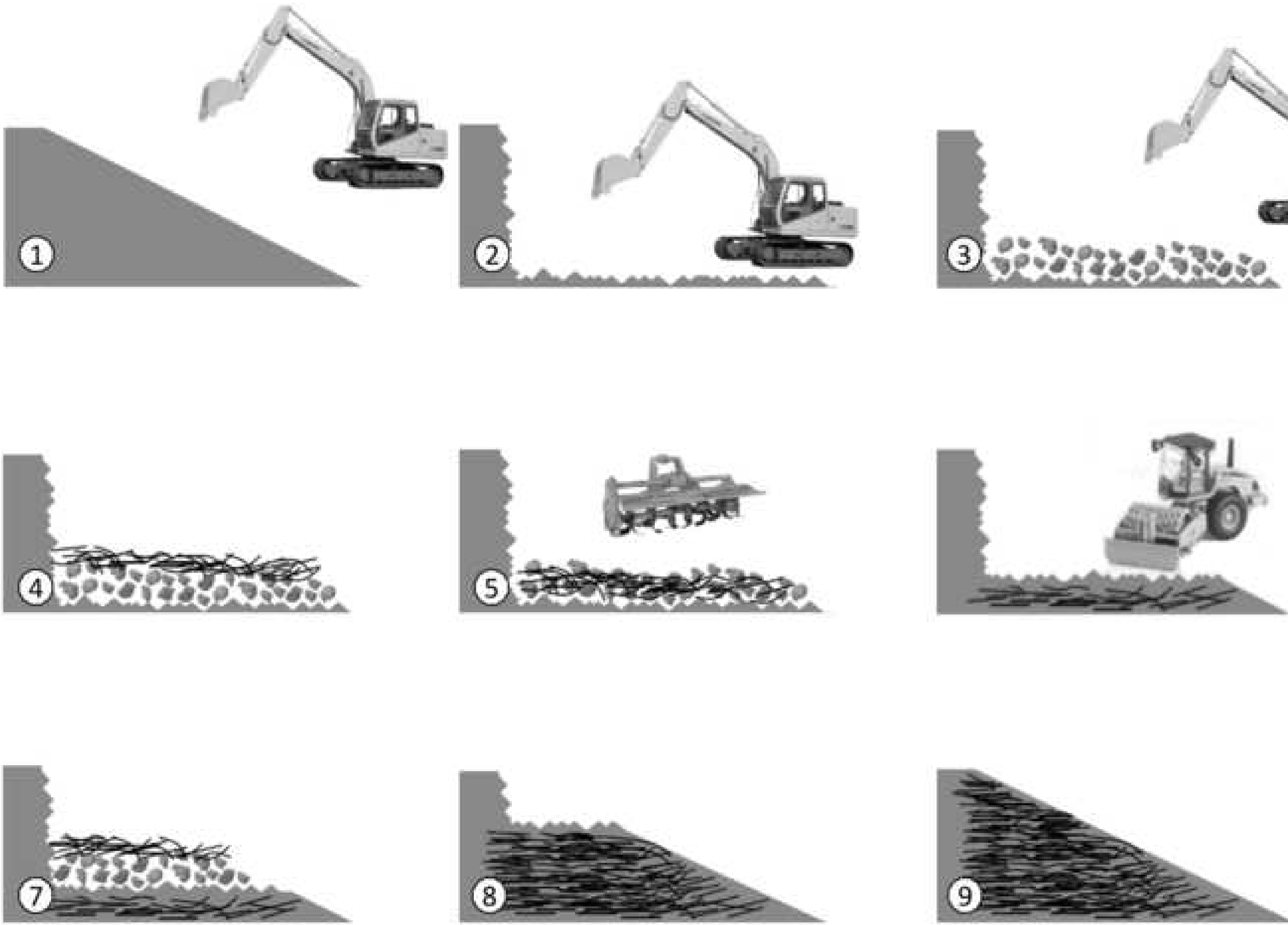

Figure 2

Click here to access/download;Figure;Ekinci Fig. 2.jpg

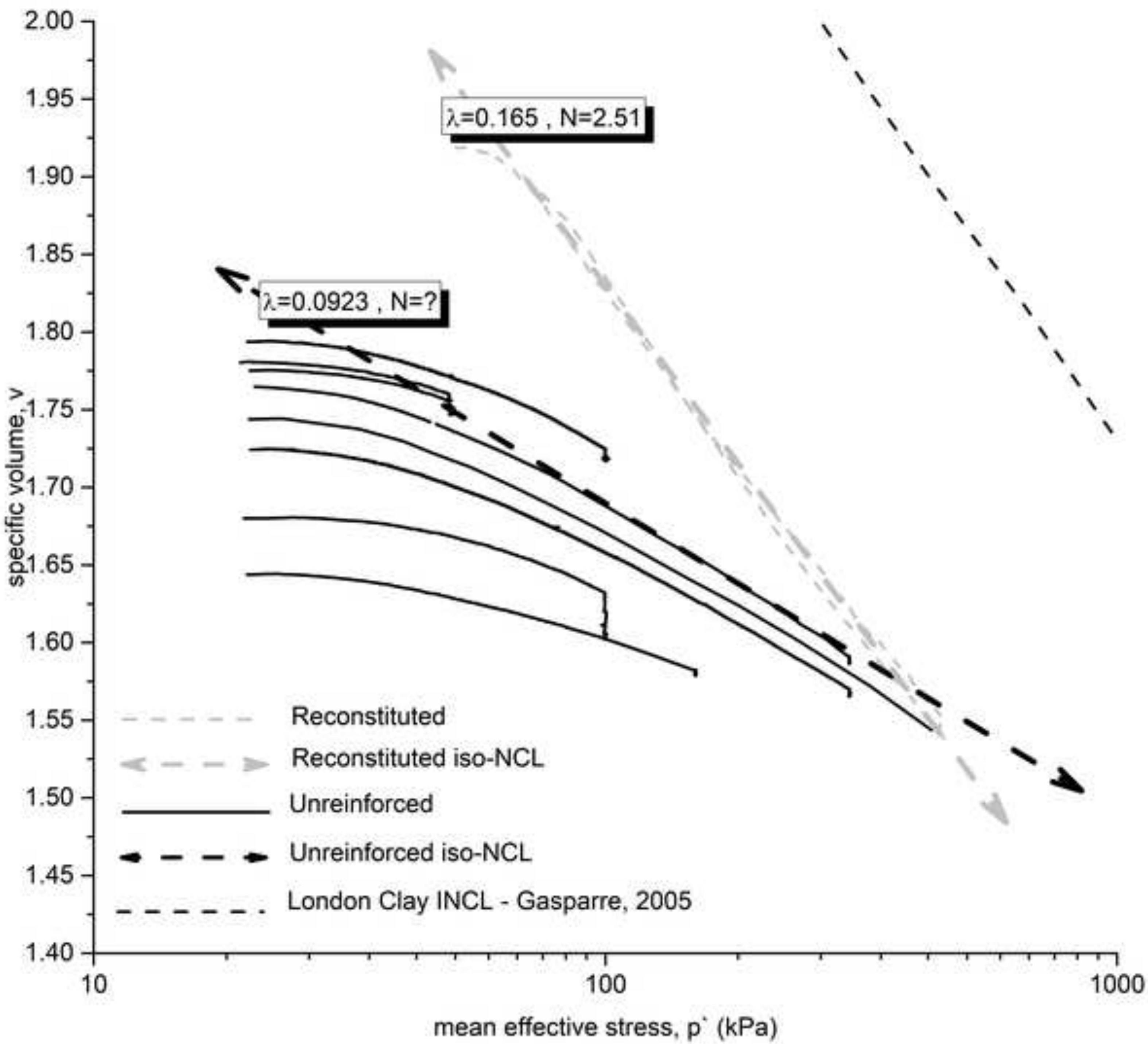
λ=0.165 , N=2.51
λ=0.0923 , N=?
2.00
1.95
1.90
1.85
1.80
1.75
1.70
1.65
1.60
1.55
1.50
1.45
1.40
specific volume, v
10
100
1000
mean effective stress, p' (kPa)
Reconstituted
Reconstituted iso-NCL
Unreinforced
Unreinforced iso-NCL
London Clay INCL - Gasparre, 2005

Figure 4

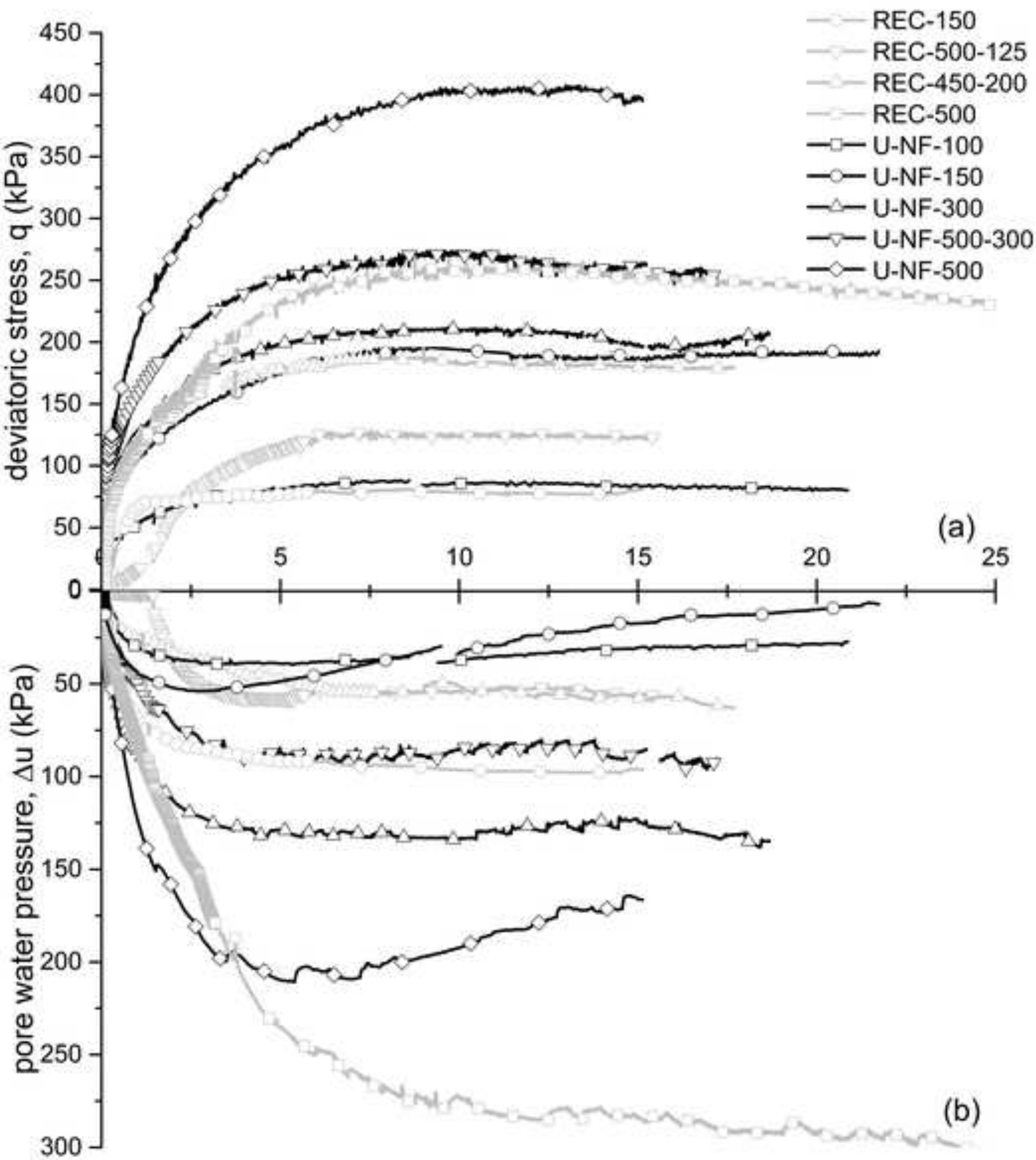
REC-150
REC-500-125
REC-450-200
REC-500
U-NF-100
U-NF-150
U-NF-300
U-NF-500-300
U-NF-500
deviatoric stress, q (kPa)
450
400
350
300
250
200
150
100
50
0
5
10
15
20
25
(a)
pore water pressure, Δu (kPa)
50
100
150
200
250
300
(b)

Figure 5 Click here to access/download;Figure;Ekinci Fig. 5B.jpg

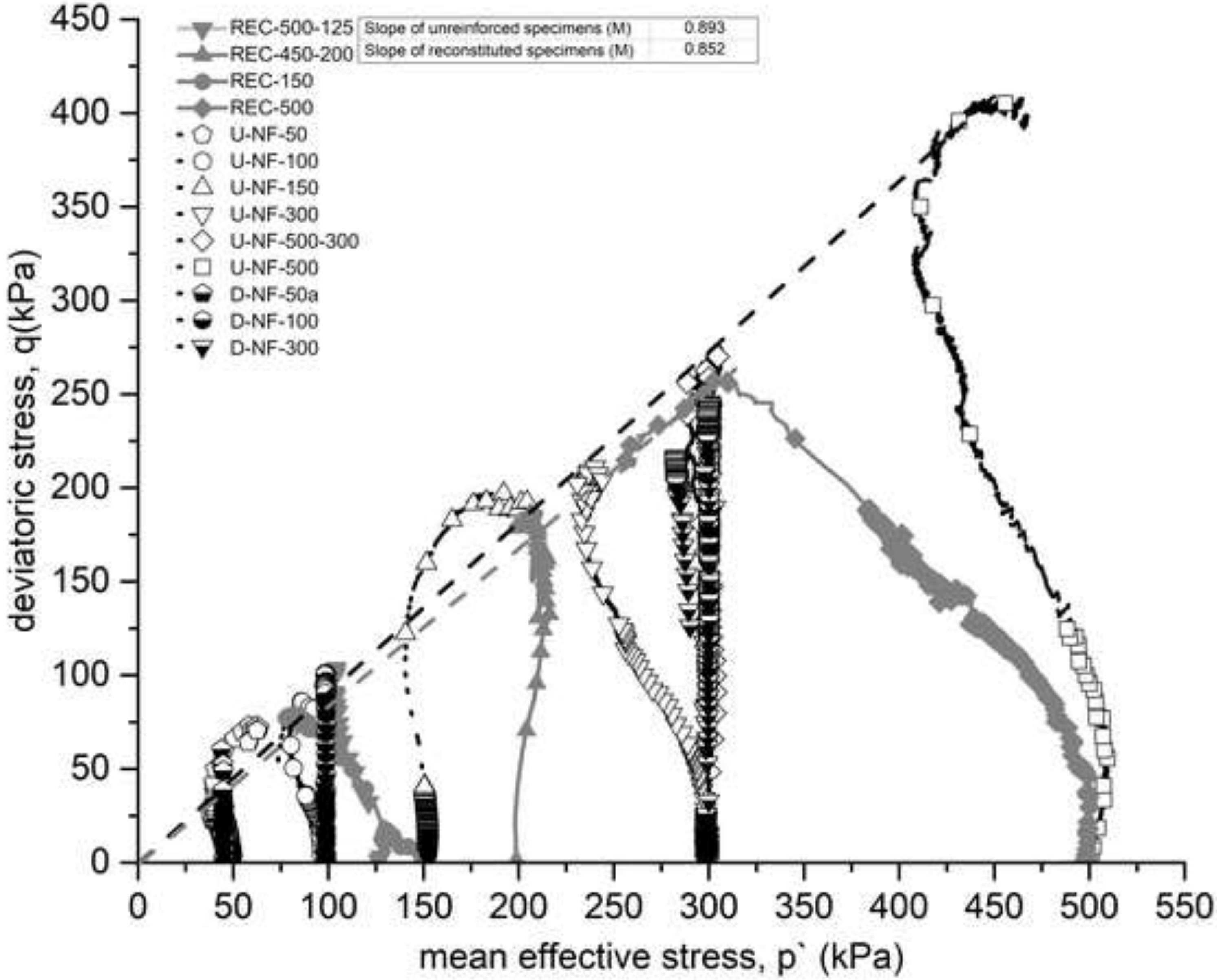

Figure 6

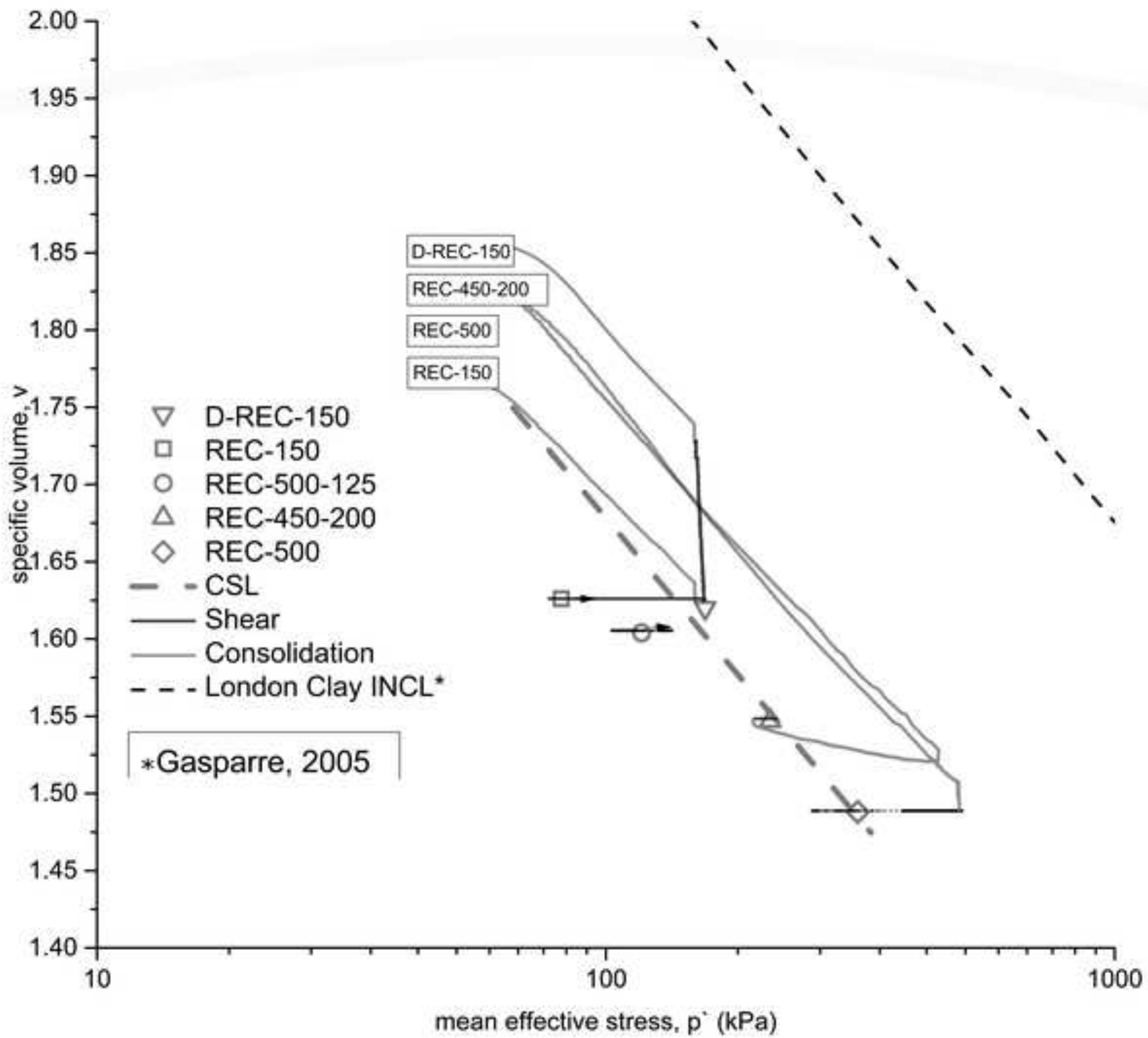

2.00
1.95
1.90
1.85
1.80
1.75
1.70
1.65
1.60
1.55
1.50
1.45
1.40
specific volume, v
10
100
1000
mean effective stress, p` (kPa)
D-REC-150
REC-450-200
REC-500
REC-150
D-REC-150
REC-150
REC-500-125
REC-450-200
REC-500
CSL
Shear
Consolidation
London Clay INCL*
*Gasparre, 2005

Figure 7

Click here to access/download;Figure;Ekinci Fig. 7.jpg

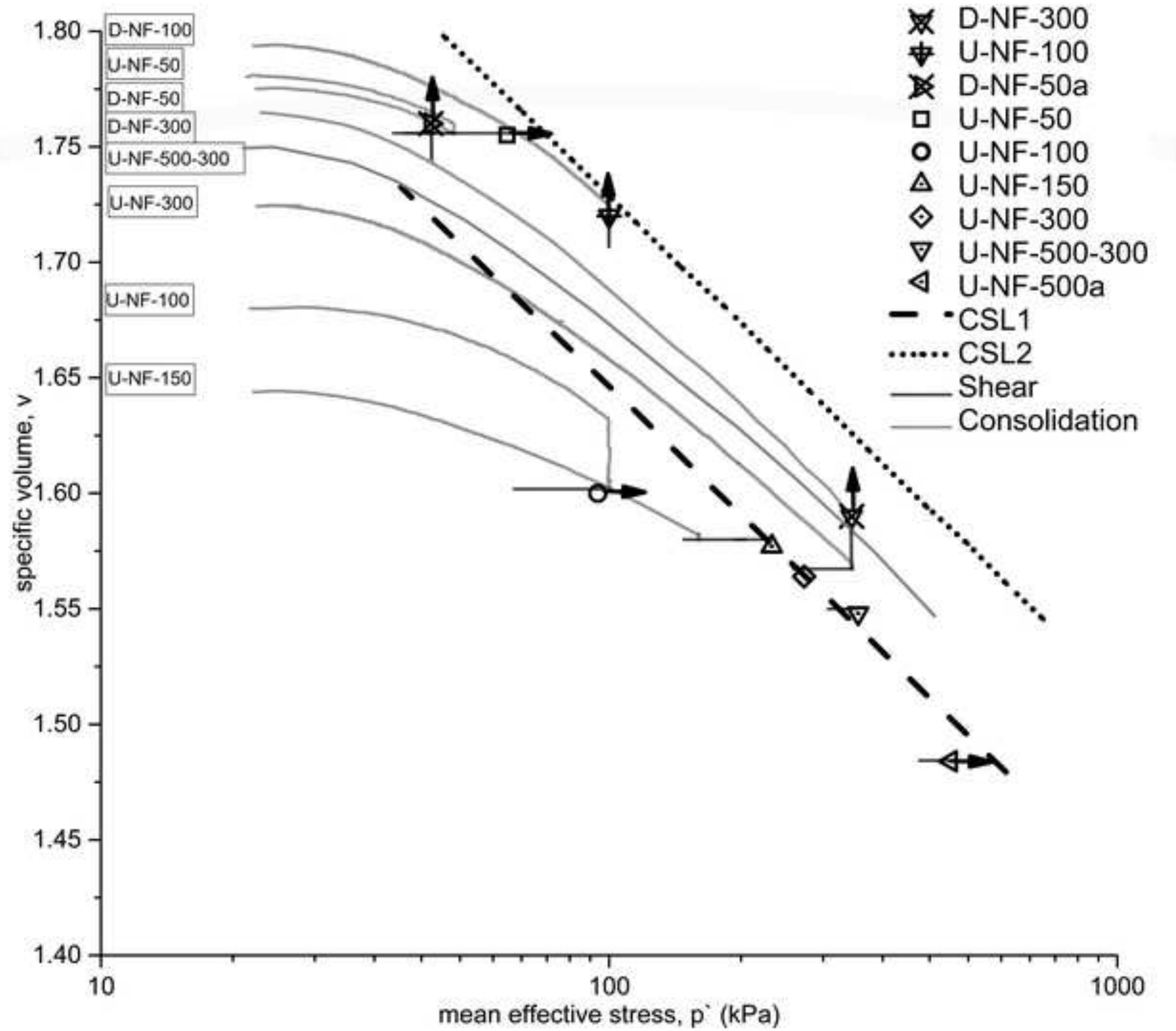

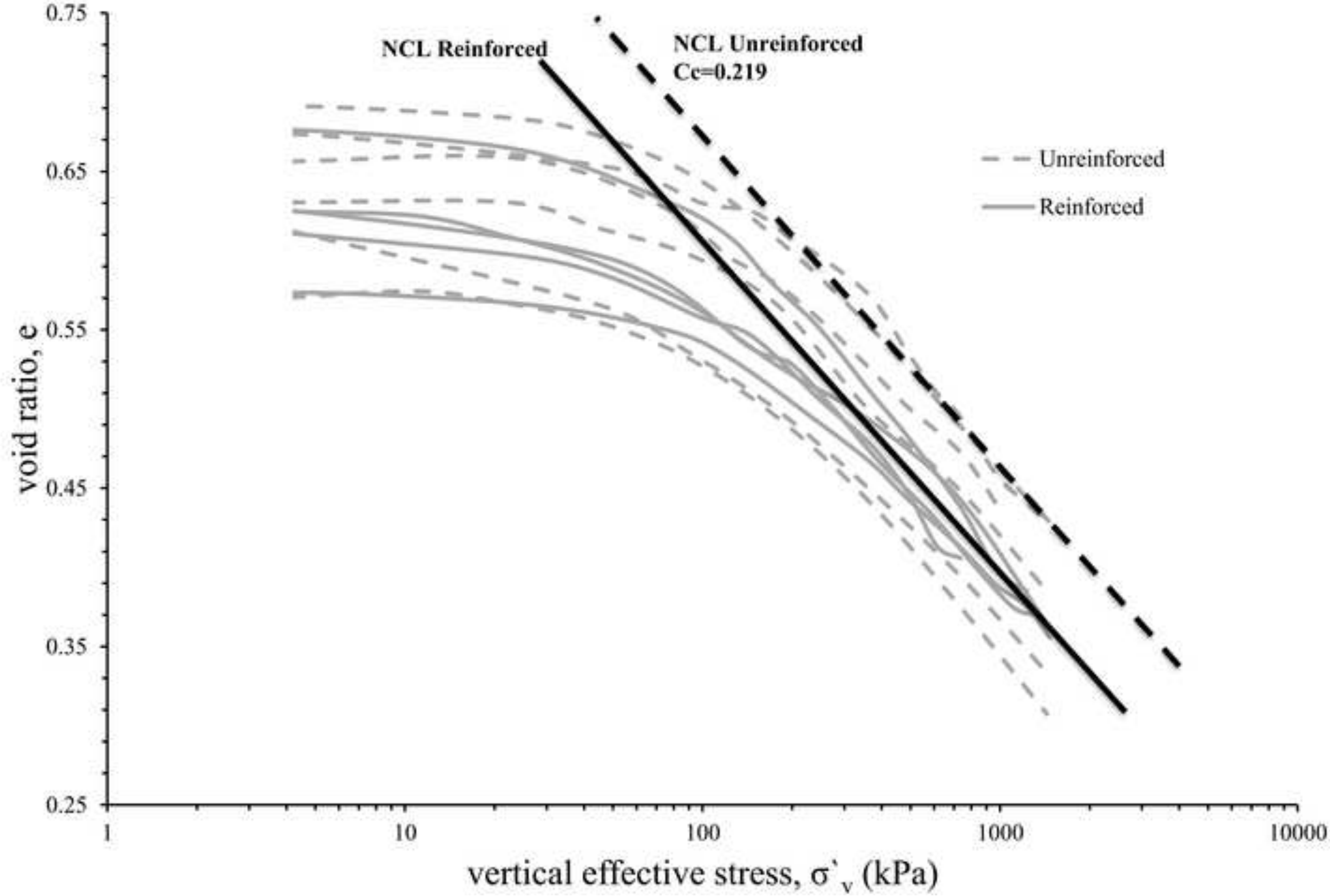

NCL Reinforced
NCL Unreinforced
Cc=0.219
Unreinforced
Reinforced
void ratio, e
0.75
0.65
0.55
0.45
0.35
0.25
1
10
100
1000
10000
vertical effective stress, σ`v (kPa)

Figure

Click here to access/download;Figure;Ekinci Fig. 9.jpg

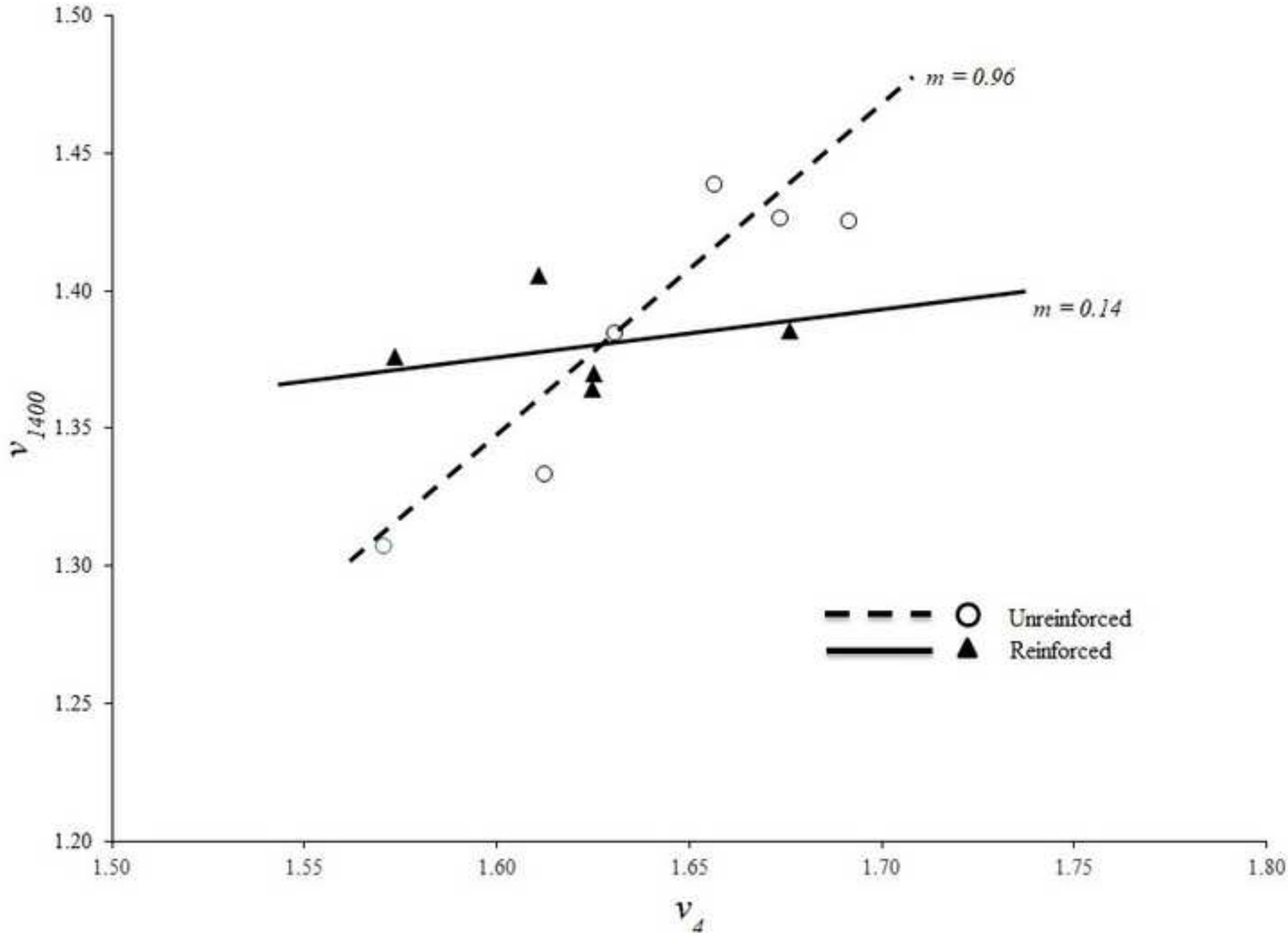

Figure 10

Click here to access/download;Figure;Ekinci Fig. 10B.jpg

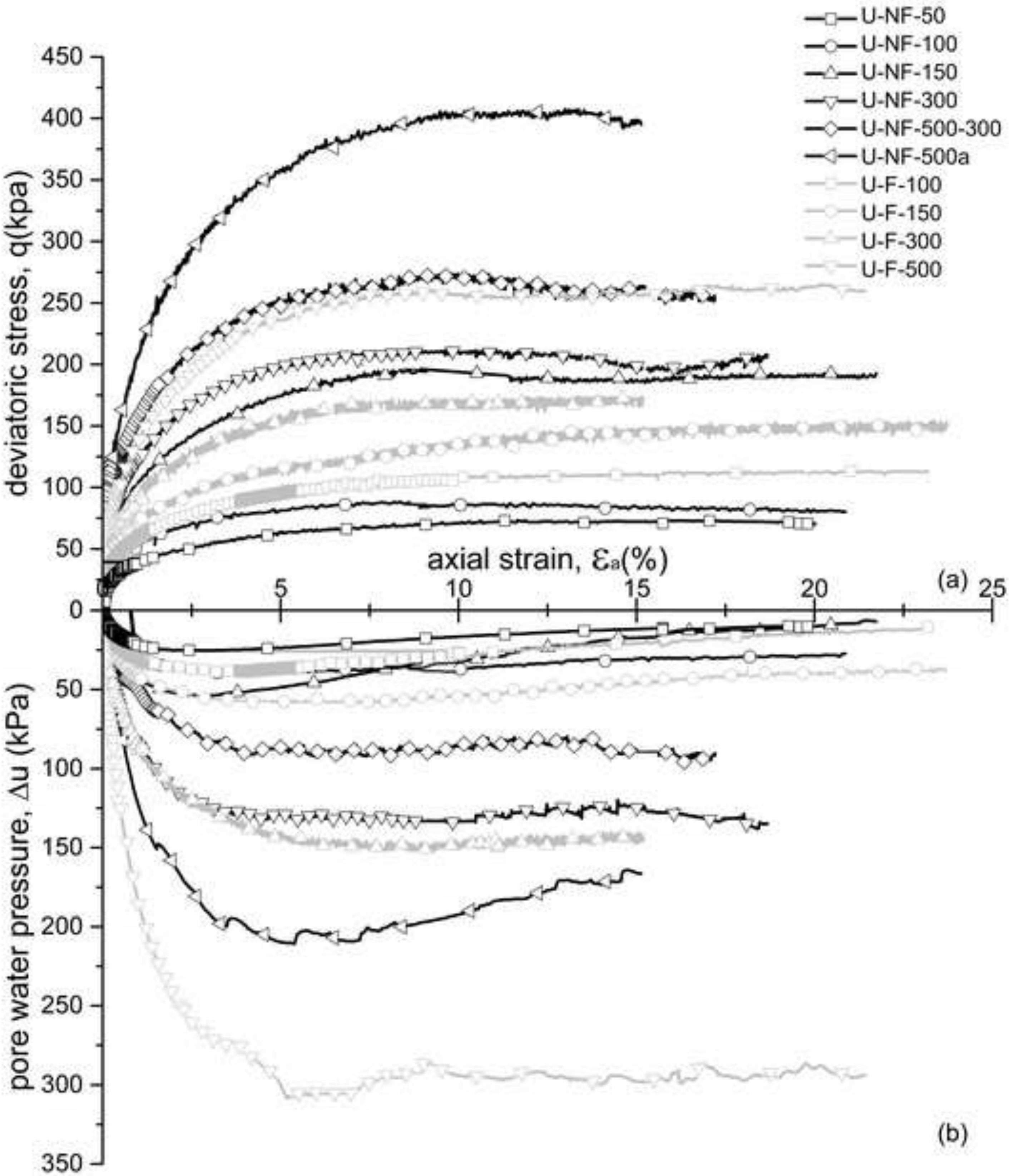

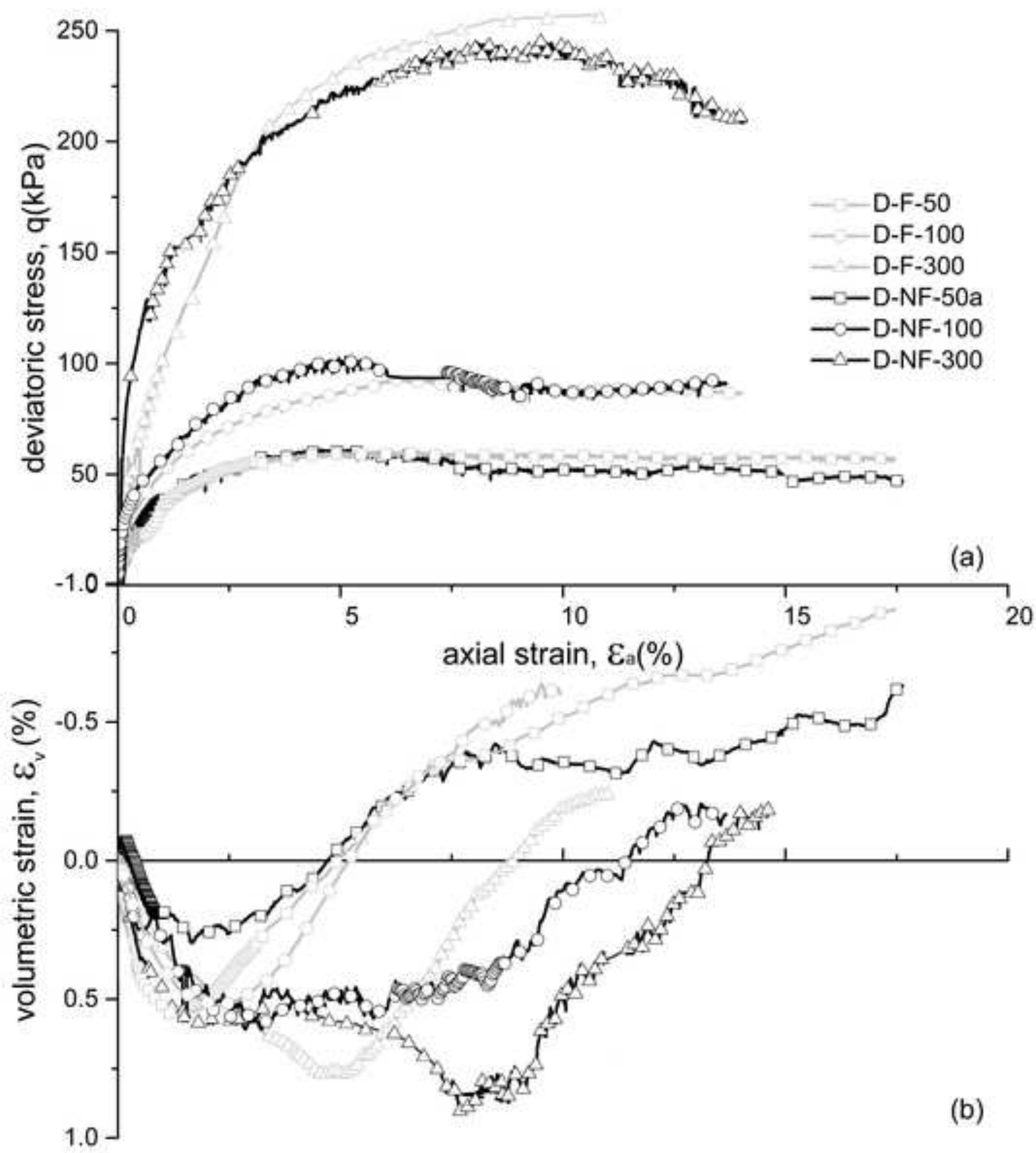
deviatoric stress, q(kPa)
250
200
150
100
50
-1.0
D-F-50
D-F-100
D-F-300
D-NF-50a
D-NF-100
D-NF-300
(a)
0
5
10
15
20
axial strain, εa(%)
volumetric strain, εv (%)
-0.5
0.0
0.5
1.0
(b)

Figure 12

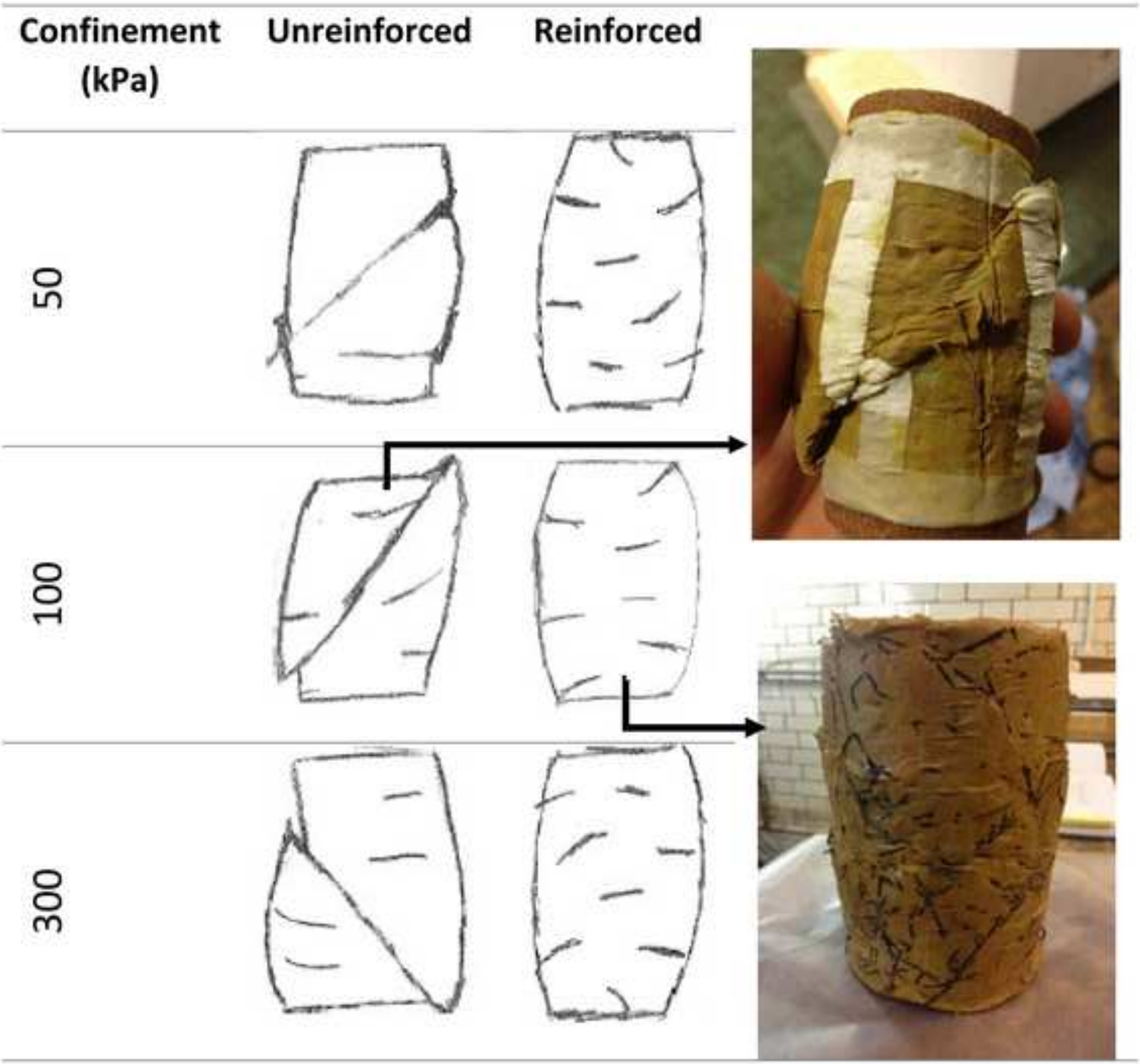

Figure 13

Click here to access/download;Figure;Ekinci Fig. 13.jpg

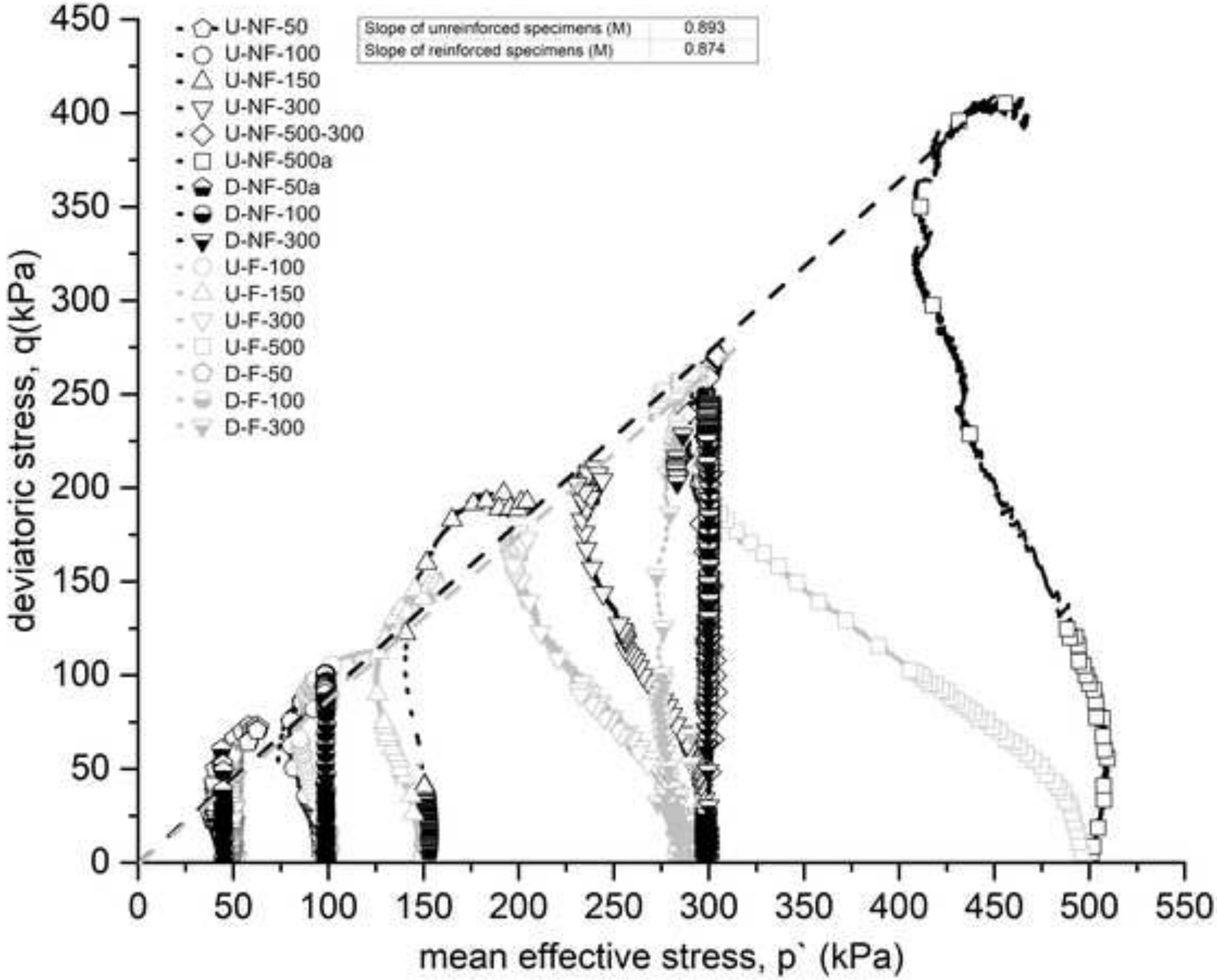

Figure 14

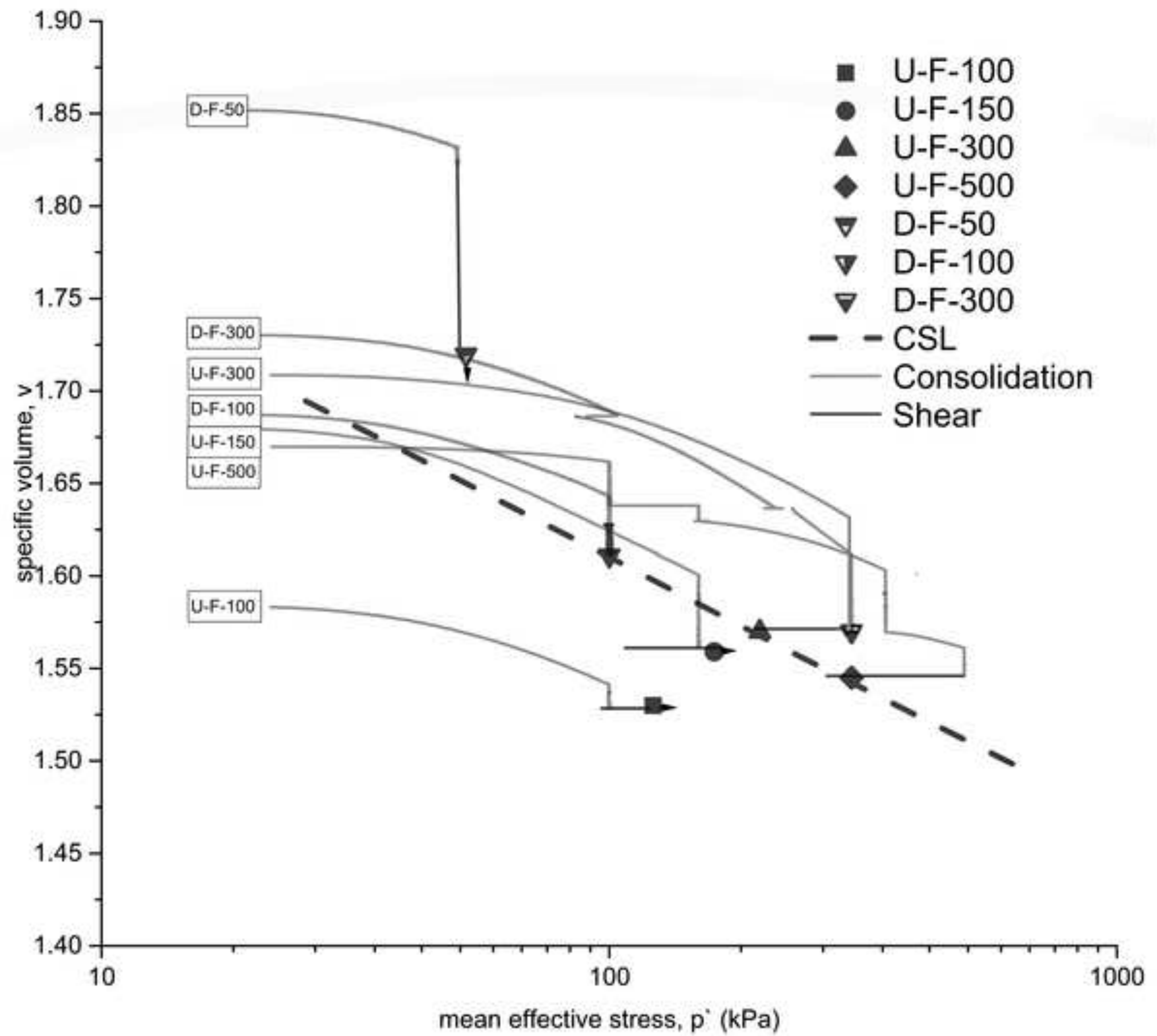

1.90
1.85
1.80
1.75
1.70
1.65
1.60
1.55
1.50
1.45
1.40
specific volume, v
10
100
1000
mean effective stress, p' (kPa)
D-F-50
D-F-300
U-F-300
D-F-100
U-F-150
U-F-500
U-F-100
U-F-100
U-F-150
U-F-300
U-F-500
D-F-50
D-F-100
D-F-300
CSL
Consolidation
Shear

Figure 15

Click here to access/download;Figure;Ekinci Fig. 15.jpg

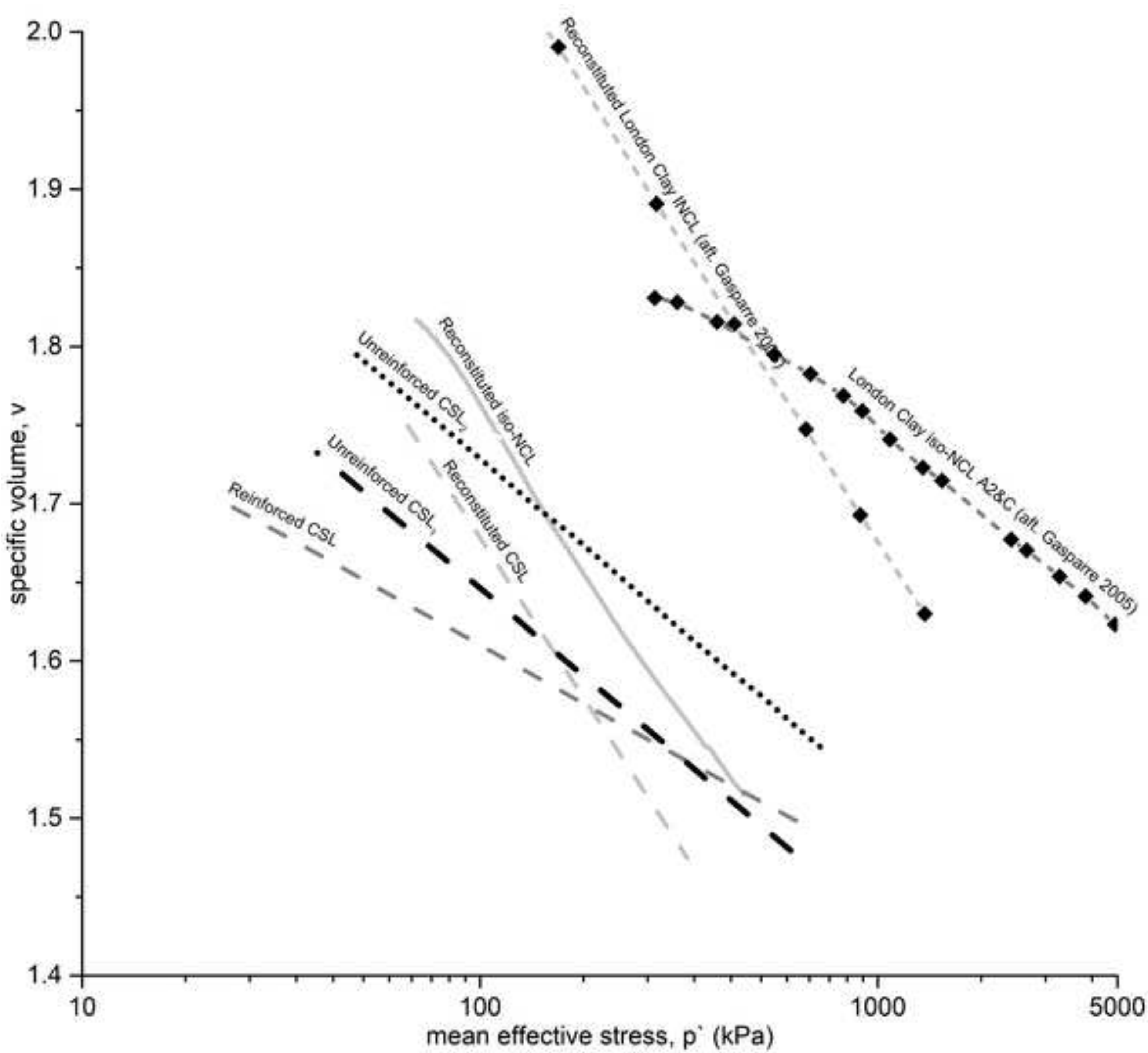

Figure 16

Click here to access/download;Figure;Ekinci Fig. 16.jpg

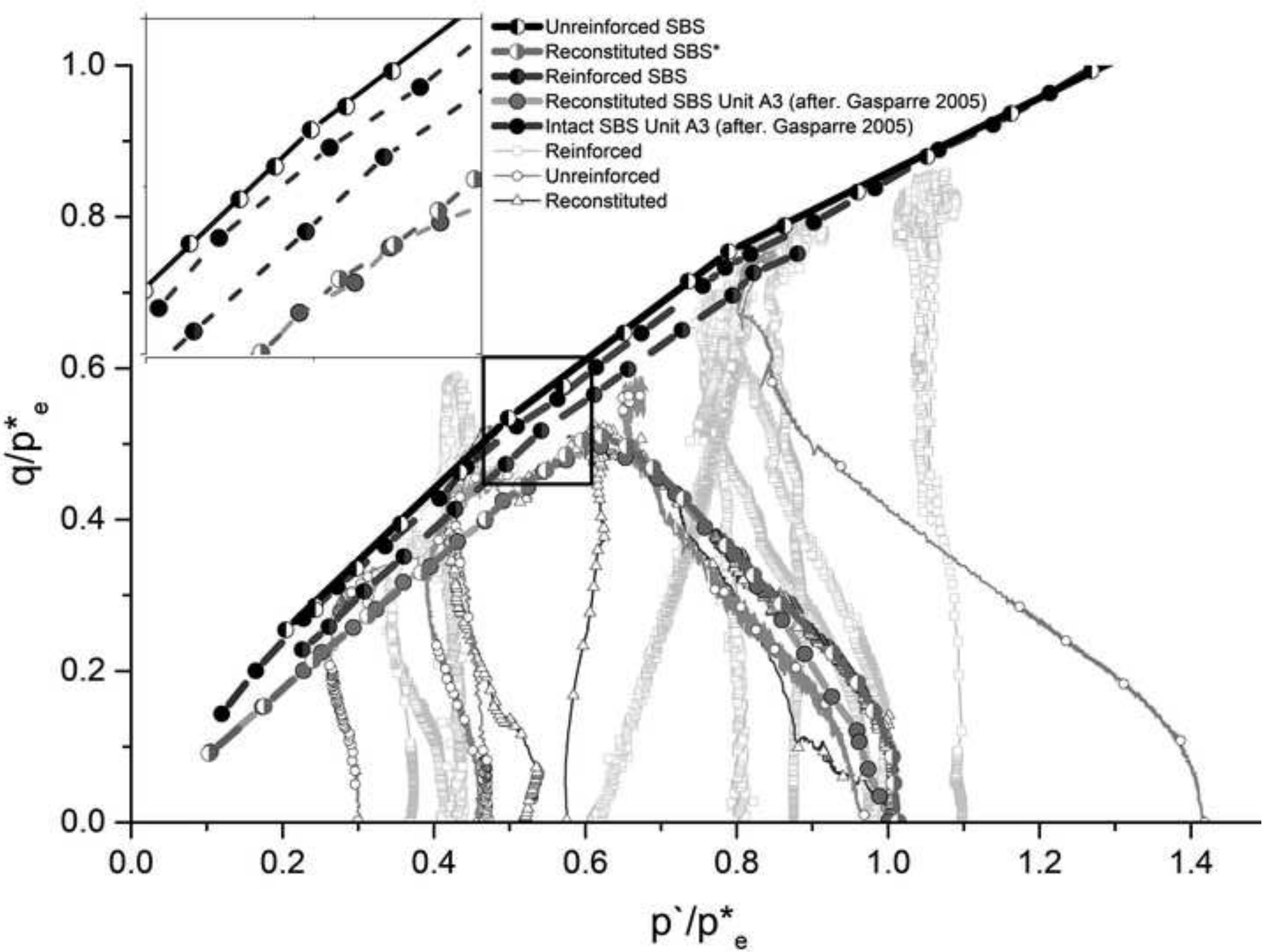

Table 1. Properties of fibres

Properties	Values
Specific gravity	0.91 g/cm^3
Denier	2610 (g/9000m)
Breaking tensile strength	350MPa
Modulus of elasticity	3500MPa
Melting point	165 °C
Burning point	590 °C
Acid and alkali resistance	Very good
Dispensability	Excellent
Moisture absorption	0%
Breaking elongation	18%
Thermal conductivity	Low
Electrical conductivity	Low
Colour	Brown

Table 2. Summary of all triaxial tests

Short Names	Diameter	Initial Void Ratio	Error in Void Ratio	Mass	Moisture Content	Density	Confinement	Pre-Shear Volumetric State
	(mm)			g	(%)	(kg/m3)	(kPa)	
D-REC-150	38	1.01	0.010	144.66	40.96	17.39	150	Dry
REC-150	38	1	0.013	153	46.67	18.12	150	Dry
REC-450-200[1]	38	0.89	0.010	155	36.92	17.02	450_200	Dry
REC-500-125[1]	38	0.86	0.011	154	35.92	18	500_125	Dry
REC-500	38	0.92	0.013	149.68	37.77	17.73	500	Wet
D-NF-50	37.62	0.56	0.017	174.63	23.3	19.56	50	Dry
D-NF-50a	39.21	0.62	0.017	183.57	26	19.21	50	Dry
D-NF-100	38.21	0.66	0.012	175.36	28.1	19.08	100	Dry
D-NF-300	37.8	0.58	0.008	177.54	27.95	20	300	Dry
U-NF-50	38.87	0.68	0.020	176.44	27.49	18.71	50	Dry
U-NF-100	39	0.59	0.014	183.08	24.26	19.27	100	Dry
U-NF-150	38.97	0.53	0.013	188.43	23	19.85	150	Dry
U-NF-300	38.2	0.55	0.013	185.36	25.3	19.96	300	Wet
U-NF-500-300[2]	37.59	0.59	0.021	172.15	27.36	19.76	500_300	Dry
U-NF-500a	38.99	0.63	0.009	181.92	24.28	18.85	500	Dry
D-F-50	105.68	0.69	0.014	3410	30.71	19.11	50	Wet
D-F-100	104.8	0.58	0.020	3455	25.1	19.64	100	Wet
D-F-300	104.96	0.65	0.012	3361	26.84	19.07	300	Wet
U-F-100	101.12	0.48	0.015	3455	26.47	21.09	100	Dry
U-F-150	101	0.42	0.011	3474.5	21.67	21.26	150	Dry
U-F-300	105	0.62	0.020	3400	25.85	19.25	300	Wet
U-F-500	105.22	0.55	0.016	3500	24.4	19.84	500	Wet
U-NF-100a	101.03	0.64	0.010	3207	29.61	19.61	100	Dry

D - Drained, U- Undrained, F - Fibres, NF - No Fibres, REC- Reconstituted, 100 – Confinement pressure
For example, D-NF-100 sample is prepared in laboratory, no fiber included, consolidated to 100 kPa and sheared in drained condition

[1] REC-500-125 (or REC-450-200) specimen prepared in the laboratory, in reconstituted state, that was consolidated to 500 kPa initially and reduced to 125 kPa to achieve over-consolidation (OCR>1) and sheared in undrained condition.
[2] U-NF-500-300 sample is prepared in laboratory, no fiber included, consolidated to 500 kPa initially and reduced to 300 kPa to achieve over-consolidation (OCR>1) and sheared in drained condition.

Table 3. Specifications of 1-D Compression tests carried out for proposed study

Sample	Diameter (mm)	Height (mm)	Mass (g)	Moisture Content (%)	Initial Void Ratio
Reinforced 1	74.60	19.95	178	24.03	0.63
Reinforced 2	74.83	39.03	361	22.70	0.56
Reinforced 3	74.82	39.03	346	24.69	0.67
Reinforced 4	74.83	39.02	357	24.80	0.61
Reinforced 5	74.82	39.04	354	24.80	0.62
Unreinforced 1	74.60	19.92	180	23.67	0.57
Unreinforced 2	74.60	19.93	180	23.32	0.61
Unreinforced 3	74.50	19.94	177	23.32	0.63
Unreinforced 4	74.83	39.04	347	28.30	0.66
Unreinforced 5	74.82	39.03	346	24.81	0.68
Unreinforced 6	74.84	39.04	352	28.14	0.65

Table 4. CSL and NCL parameters for the lines on Fig. 14

Soil	N	Γ	λ	M
Reconstituted CSL	-		0.165	0.85
Reconstituted NCL	2.51	2.498	0.165	-
Unreinforced CSL_1	-	2.071	0.092	0.89
Unreinforced CSL_2	-	2.157	0.092	0.89
Reinforced CSL	-	1.893	0.061	0.87
Reconstituted London Clay INCL*	2.83	-	0.168	0.85
London Clay iso-NCL A2&C*	-	-	0.092	-

*(after. Gasparre 2005)

THE MECHANICAL BEHAVIOUR OF COMPACTED LAMBETH-GROUP CLAYS WITH AND WITHOUT FIBRE REINFORCEMENT

Highlights

- Discrete polypropylene fibres degraded the mechanical properties of the composite beyond a critical confining pressure of 100 kPa.
- Addition of fibres changed the failure mechanism from the formation of a shear plane to barreling.
- Preparation method produced a fissure pattern in the clay that introduced transitional behaviour, which reduced with addition of the fibres.
- Behaviour of unreinforced samples was observed to be similar to highly fissured clays.
- Addition of fibres to the compacted samples created fissures with higher mobility at lower friction than those in the unreinforced samples.